Anwendungen

Paul De Monte* and Boris Lohmann

Position Trajectory Tracking of a Quadrotor based on L1 Adaptive Control

Trajektorienfolgeregelung für die Position eines Quadrokopters basierend auf der L1-adaptiven Regelung

Abstract: This paper presents an adaptive backstepping controller for the position trajectory tracking of a quadrotor. The design adopts and modifies the L1 adaptive control approach for nonlinear reference systems to fit into the backstepping design and to decouple the nominal controller from the adaptation. The controller compensates for all model uncertainties and all bounded disturbances within a particular frequency range. A stability criterion and verifiable bounds on the system signals are derived. Simulations and experimental tests demonstrate the powerful properties of the presented controller.

Keywords: Adaptive Control, Backstepping, Quadrotor Control.

Zusammenfassung: Dieser Beitrag stellt eine adaptive Backsteppingregelung für die Positionsfolge eines Quadrokopters vor. Der Entwurf greift den Ansatz der L1-adaptiven Regelung für nichtlineare Referenzmodelle auf, passt ihn an das Backsteppingschema an und modifiziert ihn dahingehend, so dass der nominale Regler von der Adaption entkoppelt. Der resultierende Regler ist in der Lage alle Modellunsicherheiten und alle begrenzten Störungen innerhalb einer gewissen Frequenz zu kompensieren. Es werden ein Stabilitätskriterium sowie verifizierbare Schranken für die Systemsignale hergeleitet. Simulationen und Experimente zeigen die starken Eigenschaften des vorgestellten Reglers.

Schlüsselwörter: Adaptive Regelung, Backstepping, Quadrokopter-Regelung.

***Corresponding Author: Paul De Monte,** TU München,
e-mail: paul.demonte@tum.de
Boris Lohmann: TU München

1 Introduction

In recent years, the trajectory tracking problem for quadrotors and other vertical take-off and landing vehicles (VTOLs) has become a broad field of research. Many nonlinear control techniques, such as feedback linearization [6, 9], sliding mode control [14] or forwarding [4] have been applied to VTOLs so far and they allow a wide range of flight maneuvers beyond hovering. In particular, Backstepping [13] is very well suited to the cascaded plant structure of VTOLs and is therefore often used to solve the tracking problem [5, 8].

In order to achieve a higher accuracy and robustness in the presence of model uncertainties and disturbances, adaptive control is a topical issue for VTOLs. For instance, aerodynamic effects are hard to identify and often neglected in the control designs. Thus the estimation and compensation of the aerodynamic effects [17] can be one objective, as well as the compensation for unknown model parameters [15] or constant disturbances [18].

Model reference adaptive control (MRAC) [1] is a famous and often used approach, but without additional augmentations, e.g. [2, 19], it suffers from certain drawbacks. MRAC is prone to responding to high-frequency excitations with fast adaptation leading to high gain feedback, which reduces the robustness margin when the adaptive estimates are directly used for control. The designer is therefore restricted to slow adaptation and must accept possibly large transients and slow convergence [3, 21]. Thus a fundamental question is how to realize high performance without sacrificing robustness.

L1 adaptive control [10, 11] is an extension of the state-predictor-based MRAC and transparently handles the trade-off between performance and robustness. With this approach, the designer can select a certain frequency range wherein uncertainties are canceled out. Thus the systems dynamics are not affected by high frequency excitations and actuator limitations can be met. In [7], the

L1 adaptive control theory for linear reference systems is applied to an autonomous helicopter. Therein the authors need to approximate the nonlinear system by a linear time-varying system such that the theory is applicable. This approximation restricts the maneuverability of the vehicle to a sufficiently small and feasible region of operation.

In contrast, our motivation for this work is to apply the L1 adaptive control theory to a quadrotor and to preserve a maximum of maneuverability. To this end we use the nonlinear backstepping approach, which is globally feasible, and extend it by the L1 adaptive control concept. The backstepping design inevitably results in a nonlinear time-varying error system and thus the L1 adaptive control theory for linear reference systems is not applicable. Therefore we adopt the recent development for SIMO nonlinear reference systems [20], extend it to MIMO systems and fit it into our backstepping approach. We further modify the existing theory to decouple the nominal control signals from the adaptation, despite uncertain input parameters. This is an important step for our practical implementation and is only covered by the L1 adaptive control theory with precisely known input parameters [10, 20]. For the resulting controller, we derive a sufficient condition for closed-loop stability and give upper bounds for the system's states, estimation errors and control input signals. Our controller is able to compensate for all model uncertainties and for a wide range of external disturbances. We show the powerful properties of the presented controller and its practical suitability by means of simulations and experimental results.

The remainder of this contribution is organized as follows: Section II introduces the quadrotor model used for the control design. Section III shows the backstepping control design and the integration of the L1 adaptive control concept. Section IV provides simulation and experimental results.

Special notations and definitions: The superscript $'$ is used to indicate the transpose of a vector or matrix. For signals in the time domain, we drop the argument t, whereas for signals in the frequency domain, we write the argument s. $\mathfrak{L}[.]$ denotes the Laplace-Transformation into the frequency domain and $\mathfrak{L}^{-1}[.]$ the transformation back into the time domain. $\|.\|$ refers to the Euclidean norm. $\hat{.}$ designates an estimated value and $\tilde{.}$ the corresponding estimation error, which is defined as $\tilde{a} = \hat{a} - a$. Moreover, $\|\mathbf{G}(s)\|_{\mathcal{L}_1} := \int_0^\infty \|\mathbf{g}(\tau)\| \, d\tau$, with $\mathbf{g}(t)$ being the impulse response of the system $\mathbf{G}(s)$.

2 Quadrotor model

Our quadrotor model is based on the common modeling for control of VTOLs in literature, e.g. [9, 12, 16], and is briefly discussed in the following. We consider all model parameters as uncertain and use the total thrust and the three torque components as control inputs. For a practical implementation, these inputs have to be transformed into four propeller commands depending on not exactly known parameters, such as the propeller lift, the motor efficiencies and the quadrotor geometry. To compensate for these uncertainties, we integrate the uncertain input gains κ_v and $\boldsymbol{\kappa}_\omega$ in our plant model below. The translational dynamics with respect to an inertial north-east-down coordinate frame are given by

$$\dot{\mathbf{x}} = \boldsymbol{v} \,, \tag{1}$$

$$\dot{\boldsymbol{v}} = \mathbf{f}_v + g\mathbf{e}_z + \kappa_v \, \mathbf{T} + \boldsymbol{\zeta}_v \,, \tag{2}$$

where $\mathbf{x} = [x \; y \; z]'$ and $\boldsymbol{v} = [\dot{x} \; \dot{y} \; \dot{z}]'$ represent the position and the velocity in $\mathbb{R}^3$, g is the gravity constant, $\mathbf{e}_z = [0 \; 0 \; 1]'$ is a unit vector pointing in the inertial ${}_I z$-direction and $\mathbf{T} = -T \, \mathbf{R}\mathbf{e}_z$ is the total thrust given in the inertial frame with the thrust magnitude T and the rotation matrix $\mathbf{R} \in SO(3) := \{\mathbf{R} \in \mathbb{R}^{3\times3} | \mathbf{R}'\mathbf{R} = \mathbf{I}_{3\times3}, \det(\mathbf{R}) = 1\}$ from the body-fixed into the inertial frame. The function $\mathbf{f}_v$ covers state-dependent aerodynamic effects and is assumed to be differentiable in its arguments. The additional input $\boldsymbol{\zeta}_v$ is a time-varying, differentiable and bounded external disturbance. The kinematics of the attitude parameter $\mathbf{R}$ are

$$\dot{\mathbf{R}} = \mathbf{R}\underline{\boldsymbol{\omega}} \,, \tag{3}$$

where $\boldsymbol{\omega} = [\omega_x \; \omega_y \; \omega_z]'$ is the angular velocity in the body-fixed frame and the map $\underline{} : \mathbb{R}^3 \to \mathbb{S}$ transforms a vector in $\mathbb{R}^3$ to the space of skew-symmetric matrices $\mathbb{S} := \{S \in \mathbb{R}^{3\times3} | S = -S'\}$ such that $\underline{\mathbf{a}}\mathbf{b} = \mathbf{a} \times \mathbf{b}$. In preparation for the backstepping design, it is worth mentioning that we can influence the total thrust vector by using $\boldsymbol{\omega}_{xy} = [\omega_x \; \omega_y]'$ and $\dot{T}$. This relation reads

$$\begin{aligned} \dot{\mathbf{T}} &= -\dot{T} \, \mathbf{R}\mathbf{e}_z - T\mathbf{R}\underline{\boldsymbol{\omega}}\mathbf{e}_z = -\dot{T} \, \mathbf{R}\mathbf{e}_z + T\mathbf{R}\underline{\mathbf{e}}_z\boldsymbol{\omega} \\ &= \underbrace{\mathbf{R}\begin{bmatrix} T\underline{\mathbf{e}}_{z1} & T\underline{\mathbf{e}}_{z2} & \mathbf{e}_z \end{bmatrix}}_{\mathbf{M}(\mathbf{R},T)} \begin{bmatrix} \omega_x & \omega_y & \dot{T} \end{bmatrix}' \,, \end{aligned} \tag{4}$$

where $\underline{\mathbf{e}}_{z1}$ and $\underline{\mathbf{e}}_{z2}$ are the first and second column of $\underline{\mathbf{e}}_z$. Note that $\underline{\mathbf{e}}_{z3} = [0 \; 0 \; 0]'$ and hence the angular velocity ω_z has no influence on the translational dynamics. We use ω_z to control the heading dynamics. Further, according to Euler's equations given in the body-fixed frame by

$$\dot{\boldsymbol{\omega}} = \mathbf{f}_\omega + \boldsymbol{\kappa}_\omega \boldsymbol{\tau} + \boldsymbol{\zeta}_\omega \,, \tag{5}$$

one may use the three torque components $\boldsymbol{\tau} = [\tau_x\ \tau_y\ \tau_z]'$ to access both: $\dot{\omega}_z$ for the heading control and $\dot{\boldsymbol{\omega}}_{xy}$ for the position tracking. The function $\mathbf{f}_\omega$ in (5) covers the Coriolis term and state-dependent aerodynamic effects and is assumed to be differentiable in its arguments. The additional input $\boldsymbol{\zeta}_\omega$ allows for a time-varying, differentiable and bounded external disturbances. To access the derivative $\dot{T}$ and $\ddot{T}$, we extend the model by two integrators for the thrust magnitude and select

$$\dddot{T} = u_T \tag{6}$$

instead of T as control input. Although this is not necessary for the backstepping design [8], the extension is still useful to obtain a smooth and less aggressive behavior [5] and most important, it simplifies the backstepping procedure, which in turn reduces the complexity to integrate the adaptation.

In summary, the system's states consist of the position $\mathbf{x}$, the velocity $\boldsymbol{v}$, the attitude $\mathbf{R}$, the angular velocity $\boldsymbol{\omega}$ and the extended states T and $\dot{T}$. All states are assumed to be known and the measured acceleration $\dot{\boldsymbol{v}}$ is also used for control.

3 Adaptive Trajectory Tracking Control

With the model presented above, we develop the adaptive trajectory tracking controller in this section. For ease of presentation, we drop the arguments of $\mathbf{M}(\mathbf{R}, T)$ in this section. For more information concerning the backstepping approach itself, we refer to [13].

3.1 Backstepping design

We define the position tracking error $\mathbf{z}_x = \mathbf{x} - \mathbf{x}_T$, with $\mathbf{x}_T$ being the desired trajectory, and choose the Lyapunov candidate function

$$V_x = \frac{1}{2}\mathbf{z}_x'\mathbf{z}_x\ , \tag{7}$$

in order to stabilize the origin $\mathbf{z}_x = 0$. The time derivative of V_x reads $\dot{V}_x = \mathbf{z}_x'(\boldsymbol{v} - \dot{\mathbf{x}}_T)$, which yields the desired velocity

$$\boldsymbol{v}_d = \dot{\mathbf{x}}_T + \mathbf{A}_x\mathbf{z}_x\,, \tag{8}$$

with $\mathbf{A}_x < 0$, that drives $V_x \to 0$. The resulting error dynamics are

$$\dot{\mathbf{z}}_x = \boldsymbol{v} - \dot{\mathbf{x}}_T = \mathbf{A}_x\,\mathbf{z}_x + \mathbf{z}_v \tag{9}$$

with the velocity error defined by $\mathbf{z}_v = \boldsymbol{v} - \boldsymbol{v}_d$. Next, we want $\mathbf{z}_v \to 0$ and thus extend V_x such that

$$V_v = V_x + \frac{1}{2}\mathbf{z}_v'\mathbf{z}_v \tag{10}$$

holds and obtain $\dot{V}_v = \mathbf{z}_x'\mathbf{A}_x\mathbf{z}_x + \mathbf{z}_v'(\mathbf{z}_x + \dot{\boldsymbol{v}} - \dot{\boldsymbol{v}}_d)$. For the desired acceleration, $\dot{\boldsymbol{v}}_d = \ddot{\mathbf{x}}_T + \mathbf{A}_x(\boldsymbol{v} - \dot{\mathbf{x}}_T)$ holds, and $\dot{\boldsymbol{v}}$ can be influenced by the thrust vector $\mathbf{T}$ referred to (2). To account for the uncertainties in (2), we formulate the error dynamics for $\mathbf{z}_v$, according to the L1 adaptive control concept, in the following way

$$\dot{\mathbf{z}}_v = \dot{\boldsymbol{v}} - \dot{\boldsymbol{v}}_d = \mathbf{A}_v\mathbf{z}_v - \mathbf{z}_x + \hat{\kappa}_v\mathbf{z}_t + \kappa_v\mathbf{T}_d + \boldsymbol{\sigma}_{vn} + \boldsymbol{\sigma}_{va}\,, \tag{11}$$

with $\mathbf{z}_t = \mathbf{T} - \mathbf{T}_d$, $\mathbf{A}_v < 0$ and $\hat{\kappa}_v$ being an estimate for κ_v. All nominal control signals as well as our estimated plant parameters are contained in $\boldsymbol{\sigma}_{vn}$, which reads

$$\boldsymbol{\sigma}_{vn} = \hat{\mathbf{f}}_v + \hat{g}\mathbf{e}_z - \dot{\boldsymbol{v}}_d - \mathbf{A}_v\mathbf{z}_v + \mathbf{z}_x\,. \tag{12}$$

Therein $\hat{\mathbf{f}}_v = \hat{\mathbf{D}}\boldsymbol{v}$ is our estimate for $\mathbf{f}_v$, with a constant matrix $\hat{\mathbf{D}} < 0$, and considers linear damping. $\hat{g}$ is a constant estimate for g. The unknown disturbances and estimation errors are contained in

$$\boldsymbol{\sigma}_{va} = -\tilde{\mathbf{f}}_v - \tilde{g}\mathbf{e}_z + \boldsymbol{\zeta}_v - \tilde{\kappa}_v\mathbf{z}_t\,, \tag{13}$$

with $\tilde{\kappa}_v = \hat{\kappa}_v - \kappa_v$. The value for $\boldsymbol{\sigma}_{va}$ will be estimated by a state predictor, yet to be defined, and denoted by $\hat{\boldsymbol{\sigma}}_{va}$. A nonadaptive backstepping design would only consider the term $\boldsymbol{\sigma}_{vn}$ in (11) and assume $\boldsymbol{\sigma}_{va} = 0$. Due to our separation into $\boldsymbol{\sigma}_{vn}$ and $\boldsymbol{\sigma}_{va}$, we sustain the nominal backstepping structure and decouple the nominal control signals from the adaptation.

Next, we divide the desired thrust into two parts such that $\mathbf{T}_d = \mathbf{T}_{da} + \mathbf{T}_{dn}$ holds and desire $\mathbf{T}_{dn} = -\kappa_v^{-1}\boldsymbol{\sigma}_{vn}$ and $\mathbf{T}_{da} = -\kappa_v^{-1}\boldsymbol{\sigma}_{va}$ in order to drive V_v to zero. Since we only know the estimate $\hat{\boldsymbol{\sigma}}_{va}$ and $\hat{\kappa}_v$ and since we intend to solely compensate for uncertainties in a lower frequency range, which is part of the L1 adaptive control concept, we assign for $\mathbf{T}_{da}$ implicitly in the frequency range: $\mathbf{T}_{da}(s) = -d_v(s)\left(\hat{\kappa}_v\mathbf{T}_{da}(s) + \hat{\boldsymbol{\sigma}}_{va}(s)\right)$. This defines a transfer function from $\hat{\boldsymbol{\sigma}}_{va}(s)$ to $\mathbf{T}_{da}(s)$ and we tune it by $d_v(s)$ to have low-pass character. In short, we write: $\mathbf{T}_{da}(s) = -\kappa_v^{-1}\hat{\boldsymbol{\eta}}_{va}(s)$, which can be expressed by the following two different ways, both required throughout this paper. With the transfer functions $\hat{\mathbf{C}}_v(s)$ and $\mathbf{C}_v(s)$, defined by

$$\hat{\mathbf{C}}_v(s) = \hat{\kappa}_v(1 + d_v(s)\hat{\kappa}_v)^{-1}d_v(s)\,\mathbf{I}_{3\times3}\,, \tag{14}$$

$$\mathbf{C}_v(s) = \kappa_v(1 + d_v(s)\kappa_v)^{-1}d_v(s)\,\mathbf{I}_{3\times3}\,, \tag{15}$$

where the initial states are set to zero, we obtain on the one hand

$$\begin{aligned}\mathbf{T}_{da}(s) &= -\hat{\kappa}_v^{-1}\hat{\mathbf{C}}_v(s)\,\hat{\boldsymbol{\sigma}}_{va}(s) \\ &= -\kappa_v^{-1}(\hat{\mathbf{C}}_v(s)\,\hat{\boldsymbol{\sigma}}_{va}(s) - (\hat{\kappa}_v-\kappa_v)\hat{\kappa}_v^{-1}\hat{\mathbf{C}}_v(s)\,\hat{\boldsymbol{\sigma}}_{va}(s)) \\ &= -\kappa_v^{-1}(\hat{\mathbf{C}}_v(s)\,\hat{\boldsymbol{\sigma}}_{va}(s) - \tilde{\kappa}_v\mathbf{T}_{da}(s)) =: -\kappa_v^{-1}\hat{\boldsymbol{\eta}}_{va}(s)\end{aligned} \tag{16}$$

and on the other hand

$$\begin{aligned}\mathbf{T}_{da}(s) &= -d_v(s)(\kappa_v\mathbf{T}_{da}(s) + \hat{\boldsymbol{\sigma}}_{va}(s) + \tilde{\kappa}_v\mathbf{T}_{da}(s)) \\ &= -\kappa_v^{-1}\mathbf{C}_v(s)\left[\hat{\boldsymbol{\sigma}}_{va}(s)+\tilde{\kappa}_v\mathbf{T}_{da}(s)\right] =: -\kappa_v^{-1}\hat{\boldsymbol{\eta}}_{va}(s)\,.\end{aligned} \tag{17}$$

We realize low-pass filters of fourth order for $\hat{\mathbf{C}}_v(s)$ and $\mathbf{C}_v(s)$, which is necessary to provide the correct and continuous derivatives $\dot{\mathbf{T}}_{da}$, $\ddot{\mathbf{T}}_{da}$ and $\dddot{\mathbf{T}}_{da}$ required for the subsequent backstepping design and the stability analysis. For the second thrust component we assign

$$\mathbf{T}_{dn} = -\hat{\kappa}_v^{-1}\boldsymbol{\sigma}_{vn} = -\kappa_v^{-1}(\boldsymbol{\sigma}_{vn}+\tilde{\kappa}_v\mathbf{T}_{dn}) =: -\kappa_v^{-1}\hat{\boldsymbol{\eta}}_{vn}\,. \tag{18}$$

For the complete desired thrust, we obtain

$$\mathbf{T}_d = -\kappa_v^{-1}\hat{\boldsymbol{\eta}}_v = -\hat{\kappa}_v^{-1}\left(\mathfrak{L}^{-1}[\hat{\mathbf{C}}_v(s)\,\hat{\boldsymbol{\sigma}}_{va}(s)] + \boldsymbol{\sigma}_{vn}\right)\,, \tag{19}$$

where $\hat{\boldsymbol{\eta}}_v := \hat{\boldsymbol{\eta}}_{va} + \hat{\boldsymbol{\eta}}_{vn}$. With (19) inserted into (11) and with $\boldsymbol{\sigma}_v := \boldsymbol{\sigma}_{va} + \boldsymbol{\sigma}_{vn}$, we have

$$\dot{\mathbf{z}}_v = \dot{\boldsymbol{v}} - \dot{\boldsymbol{v}}_d = \mathbf{A}_v\mathbf{z}_v - \mathbf{z}_x + \hat{\kappa}_v\mathbf{z}_t + \boldsymbol{\sigma}_v - \hat{\boldsymbol{\eta}}_v\,. \tag{20}$$

Next, we want to drive $\mathbf{z}_t \to 0$ and extend V_v as follows

$$V_t = V_v + \frac{1}{2}\mathbf{z}_t'\mathbf{z}_t\,. \tag{21}$$

The derivative reads $\dot{V}_t = \mathbf{z}_x'\mathbf{A}_x\mathbf{z}_x + \mathbf{z}_v'\mathbf{A}_v\mathbf{z}_v + \mathbf{z}_t'(\hat{\kappa}_v\,\mathbf{z}_v + \dot{\mathbf{T}} - \dot{\mathbf{T}}_d) + \mathbf{z}_v'(\boldsymbol{\sigma}_v - \hat{\boldsymbol{\eta}}_v)$. We keep the last term $\mathbf{z}_v'(\boldsymbol{\sigma}_v - \hat{\boldsymbol{\eta}}_v)$ unchanged in the following, because it contains the remaining estimation errors and the disturbances beyond the filter frequencies of $\mathbf{C}_v(s)$, that we do not cancel out. According to (4), $\dot{\mathbf{T}}$ can be influenced by a variation of $\boldsymbol{\omega}_{xy}$ and $\dot{T}$ and since we want to drive $V_t \to 0$, we assign

$$\begin{bmatrix}\boldsymbol{\omega}_{xyd} & \dot{T}_d\end{bmatrix}' = \mathbf{M}^{-1}\left(\hat{\dot{\mathbf{T}}}_d + \mathbf{A}_t\,\mathbf{z}_t - \hat{\kappa}_v\,\mathbf{z}_v\right)\,, \tag{22}$$

with $\mathbf{A}_t < 0$. One would expect $\hat{\dot{\mathbf{T}}}_d = \dot{\mathbf{T}}_d$ in (22) and even though we could provide the correct value for $\dot{\mathbf{T}}_d$, we rather choose

$$\hat{\dot{\mathbf{T}}}_d = -\hat{\kappa}_v^{-1}\left(\mathfrak{L}^{-1}[s\hat{\mathbf{C}}_v(s)\,\hat{\boldsymbol{\sigma}}_{va}(s)] + \hat{\dot{\boldsymbol{\sigma}}}_{vn}\right)\,, \tag{23}$$

wherein $\hat{\dot{\boldsymbol{\sigma}}}_{vn}$ is a guess for $\dot{\boldsymbol{\sigma}}_{vn}$. The former reads $\hat{\dot{\boldsymbol{\sigma}}}_{vn} = \mathbf{K}\mathbf{z}_k + \mathbf{K}_e(\mathfrak{L}^{-1}[\hat{\mathbf{C}}_v(s)\hat{\boldsymbol{\sigma}}_{va}(s)] + \boldsymbol{\sigma}_{vn} + \hat{\kappa}_v\mathbf{T}_d)$, with $\mathbf{z}_k := [\mathbf{z}_x\ \mathbf{z}_v\ \mathbf{z}_t\ \dot{\mathbf{x}}_T\ \ddot{\mathbf{x}}_T]'$. The latter reads $\dot{\boldsymbol{\sigma}}_{vn} = \mathbf{K}\mathbf{z}_k + \mathbf{K}_e(\boldsymbol{\sigma}_{va} + \boldsymbol{\sigma}_{vn} + \kappa_v\mathbf{T}_d)$ and is obtained by a derivation of (12). For both, $\mathbf{K}_e = \hat{\mathbf{D}} - \mathbf{A}_v - \mathbf{A}_x^2$ holds and $\mathbf{K}$ is a known constant parameter matrix whose definition is omitted due to limited space. The use of $\hat{\dot{\boldsymbol{\sigma}}}_{vn}$ instead of $\dot{\boldsymbol{\sigma}}_{vn}$ leads to the estimation error

$$\hat{\dot{\mathbf{T}}}_d - \dot{\mathbf{T}}_d = -\hat{\kappa}_v^{-1}(\hat{\dot{\boldsymbol{\sigma}}}_{vn} - \dot{\boldsymbol{\sigma}}_{vn}) = \hat{\kappa}_v^{-1}\mathbf{K}_e(\boldsymbol{\sigma}_v - \hat{\boldsymbol{\eta}}_v) =: \Delta\dot{\mathbf{T}}_d\,. \tag{24}$$

With (4), (22) and the definition of the angular velocity error $\mathbf{z}_r = \begin{bmatrix}\boldsymbol{\omega}_{xy}' - \boldsymbol{\omega}_{xyd}' & \dot{T} - \dot{T}_d\end{bmatrix}'$, we obtain the following error dynamics for $\mathbf{z}_t$

$$\dot{\mathbf{z}}_t = \dot{\mathbf{T}} - \dot{\mathbf{T}}_d = \mathbf{A}_t\mathbf{z}_t + \mathbf{M}\,\mathbf{z}_r - \hat{\kappa}_v\mathbf{z}_v + \Delta\dot{\mathbf{T}}_d\,. \tag{25}$$

Remark 1. We deliberately produce the estimation error $\Delta\dot{\mathbf{T}}_d$ in (25) to gain the capability to provide the correct derivative $\hat{\dot{\boldsymbol{\sigma}}}_{vn}$ required in the next design steps. If we provided the correct values for $\dot{\mathbf{T}}_d$ in (22), we would not be able to obtain the correct derivative $\ddot{\boldsymbol{\sigma}}_{vn}$ and thus we would shift the estimation error into the next Backstepping stage. Then the influence of the estimation error would be nonlinear and render our stability analysis impossible.

Remark 2. Since $\mathbf{M}^{-1} = -T^{-1}\begin{bmatrix}\underline{\mathbf{e}}_{z1} & \underline{\mathbf{e}}_{z2} & \mathbf{e}_z\end{bmatrix}\mathbf{R}'$ holds, see (4), we need to avoid the singularity $T = 0$ and thus ensure that $T \geq T_{\min} > 0$. This is a common obstacle that all quadrotor position tracking controllers have to cope with. To avoid this issue, we carefully choose a bounded and sufficiently smooth trajectory, such that it is reasonable to assume in case of moderate tracking errors: $T_{\max} \geq T \geq T_{\min} > 0$.

Next, we extend V_t once more such that

$$V_\omega = V_t + \frac{1}{2}\mathbf{z}_r{}'\mathbf{z}_r\,, \tag{26}$$

to achieve $\mathbf{z}_r \to 0$. The time derivative reads $\dot{V}_\omega = \mathbf{z}_x'\mathbf{A}_x\mathbf{z}_x + \mathbf{z}_v'\mathbf{A}_v\mathbf{z}_v + \mathbf{z}_t'\mathbf{A}_t\mathbf{z}_t + \mathbf{z}_v'(\boldsymbol{\sigma}_v - \hat{\boldsymbol{\eta}}_v) + \mathbf{z}_t'\Delta\dot{\mathbf{T}}_d + \mathbf{z}_r{}'(\mathbf{M}'\,\mathbf{z}_t + [\dot{\boldsymbol{\omega}}_{xy}' - \dot{\boldsymbol{\omega}}_{xyd}'\,\ddot{T} - \dddot{T}_d]')$. To render the last term negative definite, we use the control input $u_T = \ddot{T}$ from (6) and we define a virtual variable $\boldsymbol{\omega}_{xy}$, where $\dot{\boldsymbol{\omega}}_{xy} \stackrel{!}{=} \boldsymbol{\omega}_{xy}$ is the objective for the torque inputs. Hence we choose, with $\mathbf{A}_r < 0$,

$$\begin{bmatrix}\boldsymbol{\omega}_{xy}' & u_T\end{bmatrix}' = \begin{bmatrix}\dot{\boldsymbol{\omega}}_{xyd}' & \ddot{T}_d\end{bmatrix}' + \mathbf{A}_r\,\mathbf{z}_r - \mathbf{M}'\,\mathbf{z}_t\,. \tag{27}$$

The desired derivatives therein read $[\dot{\boldsymbol{\omega}}_{xyd}'\,\dddot{T}_d]' = \dot{\mathbf{M}}^{-1}\mathbf{M}[\boldsymbol{\omega}_{xyd}'\,\dot{T}_d]' + \mathbf{M}^{-1}(\hat{\ddot{\mathbf{T}}}_d + \mathbf{A}_t\dot{\mathbf{z}}_t - \hat{\kappa}_v\dot{\mathbf{z}}_v)$, where $\hat{\ddot{\mathbf{T}}}_d(s) = -\hat{\kappa}_v^{-1}(\mathfrak{L}^{-1}[s^2\hat{\mathbf{C}}_v(s)\,\hat{\boldsymbol{\sigma}}_{va}(s)] + \hat{\ddot{\boldsymbol{\sigma}}}_{vn})$. The derivation of $\dot{\mathbf{M}}^{-1}$ is straight forward and omitted due to limited space. For the value $\hat{\ddot{\boldsymbol{\sigma}}}_{vn}$, we take advantage of the

fact that $\dot{\boldsymbol{\sigma}}_{vn} + \hat{\kappa}_v \dot{\mathbf{T}}_d = \dot{\hat{\boldsymbol{\sigma}}}_{vn} + \hat{\kappa}_v \dot{\hat{\mathbf{T}}}_d$ holds and provide $\dot{\hat{\boldsymbol{\sigma}}}_{vn} = \mathbf{K}\dot{\mathbf{z}}_k + \mathbf{K}_e(\mathfrak{L}^{-1}[s\hat{\mathbf{C}}_v(s)\hat{\boldsymbol{\sigma}}_{va}(s)] + \hat{\boldsymbol{\sigma}}_{vn} + \hat{\kappa}_v \dot{\hat{\mathbf{T}}}_d)$.

Next, we address the heading control. We realize a desired constant angular rate ω_{zd} by means of a rate controller. Since ω_z has no influence on the position tracking control, this is a suitable choice. We define the angular rate error $z_{\omega z} = \omega_z - \omega_{zd}$ and the virtual variable ω_z and desire, with $a_{\omega z} < 0$,

$$\dot{z}_{\omega z} = \dot{\omega}_z \stackrel{!}{=} \omega_z := a_{\omega z} z_{\omega z} \,. \tag{28}$$

In order to generate $\dot{\boldsymbol{\omega}}_{xy}$ from (27) and $\dot{\omega}_z$ from (28), despite of all uncertainties, we write (5) as

$$\dot{\boldsymbol{\omega}} = \boldsymbol{\omega} + \boldsymbol{\kappa}_\omega \boldsymbol{\tau} + \boldsymbol{\sigma}_{\omega n} + \boldsymbol{\sigma}_{\omega a} \,, \tag{29}$$

where $\boldsymbol{\omega} = \begin{bmatrix} \boldsymbol{\omega}'_{xy} & \omega_z \end{bmatrix}'$ holds and $\boldsymbol{\sigma}_{\omega n}$ contains all known values, whereas $\boldsymbol{\sigma}_{\omega a}$ contains all uncertain values except the input gain matrix $\boldsymbol{\kappa}_\omega$. Both read

$$\boldsymbol{\sigma}_{\omega n} = \hat{\mathbf{f}}_\omega - \boldsymbol{\omega} \,, \quad \boldsymbol{\sigma}_{\omega a} = -\tilde{\mathbf{f}}_\omega + \boldsymbol{\zeta}_\omega \,, \tag{30}$$

where $\hat{\mathbf{f}}_\omega = \hat{\mathbf{J}}^{-1}(\hat{\mathbf{J}}\boldsymbol{\omega} \times \boldsymbol{\omega})$ is our estimate for the Coriolis term. Similar to the desired thrust definition, we divide the control torques into two components such that $\boldsymbol{\tau} = \boldsymbol{\tau}_a + \boldsymbol{\tau}_n$ holds and define similar to (16) and (17)

$$\begin{aligned} \boldsymbol{\tau}_a(s) &= -\hat{\boldsymbol{\kappa}}_\omega^{-1} \hat{\mathbf{C}}_\omega(s)\, \hat{\boldsymbol{\sigma}}_{\omega a}(s) \qquad (31)\\ &= -\boldsymbol{\kappa}_\omega^{-1}(\hat{\mathbf{C}}_\omega(s)\, \hat{\boldsymbol{\sigma}}_{\omega a}(s) - \tilde{\boldsymbol{\kappa}}_\omega \boldsymbol{\tau}_a(s)) =: -\boldsymbol{\kappa}_\omega^{-1} \hat{\boldsymbol{\eta}}_{\omega a}(s) \,, \\ \boldsymbol{\tau}_a(s) &= -d_\omega(s)(\boldsymbol{\kappa}_\omega \boldsymbol{\tau}_a(s) + \hat{\boldsymbol{\sigma}}_{\omega a}(s) + \tilde{\boldsymbol{\kappa}}_\omega \boldsymbol{\tau}_a(s)) \qquad (32)\\ &= -\boldsymbol{\kappa}_\omega^{-1} \mathbf{C}_\omega(s) \left[\hat{\boldsymbol{\sigma}}_{\omega a}(s) + \tilde{\boldsymbol{\kappa}}_\omega \boldsymbol{\tau}_a(s)\right] =: -\boldsymbol{\kappa}_\omega^{-1} \hat{\boldsymbol{\eta}}_{\omega a}(s) \,. \end{aligned}$$

The transfer functions $\hat{\mathbf{C}}_{\omega a}(s)$ and $\mathbf{C}_{\omega a}(s)$ read

$$\hat{\mathbf{C}}_\omega(s) = \hat{\boldsymbol{\kappa}}_\omega(\mathbf{I}_{3\times 3} + \mathbf{d}_\omega(s)\hat{\boldsymbol{\kappa}}_\omega)^{-1}\mathbf{d}_\omega(s) \,, \tag{33}$$

$$\mathbf{C}_\omega(s) = \boldsymbol{\kappa}_\omega(\mathbf{I}_{3\times 3} + \mathbf{d}_\omega(s)\boldsymbol{\kappa}_\omega)^{-1}\mathbf{d}_\omega(s) \,, \tag{34}$$

with the initial values set to zero. For the second torque component we define

$$\boldsymbol{\tau}_n = -\hat{\boldsymbol{\kappa}}_\omega^{-1}\boldsymbol{\sigma}_{\omega n} = -\boldsymbol{\kappa}_\omega^{-1}(\boldsymbol{\sigma}_{\omega n} + \tilde{\boldsymbol{\kappa}}_\omega \boldsymbol{\tau}_n) =: -\boldsymbol{\kappa}_\omega^{-1}\hat{\boldsymbol{\eta}}_{\omega n} \,. \tag{35}$$

For the complete torque, with $\hat{\boldsymbol{\eta}}_\omega = \hat{\boldsymbol{\eta}}_{\omega a} + \hat{\boldsymbol{\eta}}_{\omega n}$, we obtain

$$\boldsymbol{\tau} = -\boldsymbol{\kappa}_\omega^{-1}\hat{\boldsymbol{\eta}}_\omega = -\hat{\boldsymbol{\kappa}}_\omega^{-1}\left(\mathfrak{L}^{-1}[\hat{\mathbf{C}}_\omega(s)\, \hat{\boldsymbol{\sigma}}_{\omega a}(s)] + \boldsymbol{\sigma}_{\omega n}\right) \,. \tag{36}$$

With this torque command the error dynamics for $\mathbf{z}_r$ read

$$\dot{\mathbf{z}}_r = \mathbf{A}_r \mathbf{z}_r - \mathbf{M}'\mathbf{z}_t + \mathrm{diag}(1,1,0)(\boldsymbol{\sigma}_\omega - \hat{\boldsymbol{\eta}}_\omega) \,, \tag{37}$$

with $\boldsymbol{\sigma}_\omega := \boldsymbol{\sigma}_{\omega a} + \boldsymbol{\sigma}_{\omega n}$.

The final Lyapunov candidate function for the complete system is

$$V(\mathbf{z}) = V_\omega + \frac{1}{2} z_{\omega z}{}^2 \,, \tag{38}$$

with the error state vector defined as $\mathbf{z}' = [\mathbf{z}'_x, \mathbf{z}'_v, \mathbf{z}'_t, \mathbf{z}'_r, z_{\omega z}]'$. The derivative of (38) takes the form

$$\dot{V} = \mathbf{z}'\ \mathbf{A}_V\ \mathbf{z} + \mathbf{z}'\mathbf{B}_v(\boldsymbol{\sigma}_v - \hat{\boldsymbol{\eta}}_v) + \mathbf{z}'\mathbf{B}_\omega(\boldsymbol{\sigma}_\omega - \hat{\boldsymbol{\eta}}_\omega) \,, \tag{39}$$

with $\mathbf{A}_V = \mathrm{diag}(\mathbf{A}_x, \mathbf{A}_v, \mathbf{A}_t, \mathbf{A}_r, a_{\omega z})$, (40)

$$\mathbf{B}'_v = \begin{bmatrix} \mathbf{0}_{3\times 3} & \mathbf{I}_{3\times 3} & \hat{\kappa}_v^{-1}\mathbf{K}_e & \mathbf{0}_{3\times 3} & \mathbf{0}_{3\times 1} \end{bmatrix}' \,, \tag{41}$$

$$\mathbf{B}'_\omega = \begin{bmatrix} \mathbf{0}_{3\times 3} & \mathbf{0}_{3\times 3} & \mathbf{0}_{3\times 3} & \mathrm{diag}(1,1,0) & [0\ 0\ 1]' \end{bmatrix}' \tag{42}$$

For ease of presentation, we combine and shorten the used terms by the following definitions: $\mathbf{B} := [\mathbf{B}_v\ \mathbf{B}_\omega]$ and for $l \in \{a, n\}$, $\boldsymbol{\sigma}_l := [\boldsymbol{\sigma}'_{vl}\ \boldsymbol{\sigma}'_{\omega l}]'$, $\hat{\boldsymbol{\eta}}_l := [\hat{\boldsymbol{\eta}}'_{vl}\ \hat{\boldsymbol{\eta}}'_{\omega l}]'$, $\mathbf{u}_l := [\mathbf{T}'_{dl}\ \boldsymbol{\tau}'_l]'$ and $\mathbf{C}(s) = \mathrm{diag}(\mathbf{C}_v(s), \mathbf{C}_\omega(s))$, $\tilde{\boldsymbol{\kappa}} = \mathrm{diag}(\tilde{\kappa}_v, \tilde{\boldsymbol{\kappa}}_\omega)$. With these definitions and some simplifications, (39) reads $\dot{V} = \mathbf{z}'\mathbf{A}_V\mathbf{z} + \mathbf{z}'\mathbf{B}(\boldsymbol{\sigma}_a - \hat{\boldsymbol{\eta}}_a + \tilde{\boldsymbol{\kappa}}\hat{\boldsymbol{\kappa}}^{-1}\boldsymbol{\sigma}_n)$ and the corresponding nonlinear time-varying error dynamics, obtained by the combination of (9), (20), (25), (28) and (37), are

$$\dot{\mathbf{z}} = \underbrace{\begin{bmatrix} \mathbf{A}_x\mathbf{z}_x + \mathbf{z}_v \\ -\mathbf{z}_x + \mathbf{A}_v\mathbf{z}_v + \hat{\kappa}_v\mathbf{z}_t \\ -\hat{\kappa}_v\mathbf{z}_v + \mathbf{A}_t\mathbf{z}_t + \mathbf{M}\mathbf{z}_r \\ -\mathbf{M}'\mathbf{z}_t + \mathbf{A}_r\mathbf{z}_r \\ a_{\omega z}z_{\omega z} \end{bmatrix}}_{\mathbf{f}:=\mathbf{f}(t,\mathbf{z},\hat{\boldsymbol{\eta}}_{ua})} + \mathbf{B}\left(\boldsymbol{\sigma}_a - \hat{\boldsymbol{\eta}}_a - \tilde{\boldsymbol{\kappa}}\mathbf{u}_n\right) \,, \tag{43}$$

where

$$\hat{\boldsymbol{\eta}}_a(s) = \mathbf{C}(s)(\hat{\boldsymbol{\sigma}}_a(s) - \tilde{\boldsymbol{\kappa}}\mathbf{u}_a(s)) \,, \tag{44}$$

$$[\mathbf{T}'_d\ \boldsymbol{\tau}']' = -\hat{\boldsymbol{\kappa}}^{-1}\boldsymbol{\sigma}_n - \boldsymbol{\kappa}^{-1}\hat{\boldsymbol{\eta}}_a \,. \tag{45}$$

If we had perfect estimation in the whole frequency domain and if we knew the exact input gains, i.e. $\hat{\boldsymbol{\eta}}_a = \boldsymbol{\sigma}_a$ and $\tilde{\boldsymbol{\kappa}} = \mathbf{0}$, (39) would read $\dot{V} = \mathbf{z}'\mathbf{A}_V\mathbf{z}$ and thus the nominal closed-loop system $\dot{\mathbf{z}} = \mathbf{f}(t, \mathbf{z}, \hat{\boldsymbol{\eta}}_{va})$ would be asymptotically stable. However, since we solely compensate for uncertainties in a lower frequency range and since a small estimation error always remains, further analysis is needed.

3.2 Properties of the error dynamics

The following definitions and properties of (43) are required for the subsequent analysis:

Compact sets and constants:
We define a constant ρ_{ref} to be

$$\rho_{\text{ref}} := \|\mathbf{z}_0\| + \epsilon\,, \tag{46}$$

where $\mathbf{z}(t{=}0) = \mathbf{z}_0$ are the initial values for (43) and ϵ is an arbitrary small constant. The selection of ϵ poses a certain performance specification such that the states of a reference model, yet to be defined, with $\mathbf{z}_{\text{ref}}(t{=}0){=}\mathbf{z}_0$, will, for all times, stay in the set

$$\mathcal{Z}_{\text{ref}} := \{\mathbf{z}_{\text{ref}} \in \mathbb{R}^{13} \mid \|\mathbf{z}_{\text{ref}}\| \leq \rho_{\text{ref}}\}\,. \tag{47}$$

Further, we define a second constant ρ to be

$$\rho := \rho_{\text{ref}} + \gamma\,, \tag{48}$$

where γ is also an arbitrary small constant. The selection of γ poses a certain performance specification such that the states of the closed-loop system (43) will stay in

$$\mathcal{Z} := \{\mathbf{z} \in \mathbb{R}^{13} \mid \|\mathbf{z}\| \leq \rho\}\,, \quad \forall t. \tag{49}$$

A third arbitrary small constant $\bar{\gamma}_0$ is going to serve as an upper bound for the estimation error $\tilde{\mathbf{z}}$ to be defined in Sec. 3.4. The smaller this value is chosen, the higher is the demanded adaption performance. To streamline the analysis in this contribution, we link this value to the value γ such that

$$\bar{\gamma}_0 := g_0\gamma \tag{50}$$

holds without loss of generality.

Partial knowledge of the input gains:
For the nominal system input parameter $\hat{\boldsymbol{\kappa}} = \operatorname{diag}(\hat{\kappa}_v \cdot \mathbf{I}_{3\times3}, \hat{\boldsymbol{\kappa}}_\omega)$ holds, with $\hat{\kappa}_v = \hat{m}^{-1}$ and $\hat{\boldsymbol{\kappa}}_\omega = \hat{\mathbf{J}}^{-1}$. The mass m and the inertia $\mathbf{J}$ are positive values and physically bounded away from zero. Thus $\boldsymbol{\kappa}$ is nonsingular, $\operatorname{sgn}(\kappa_{ii}) = +1$ and $\hat{\kappa}_{ij} = 0$ holds with $i \neq j$. Further, we assume that there exists a compact and convex set $\mathbb{K}$, such that we can determine the upper bounds

$$\max_{\boldsymbol{\kappa}\in\mathbb{K}}\{\left\|\boldsymbol{\kappa}^{-1}\right\|\} \leq B_\kappa\,, \quad \max_{\boldsymbol{\kappa}\in\mathbb{K}}\{\left\|\tilde{\boldsymbol{\kappa}}\hat{\boldsymbol{\kappa}}^{-1}\right\|\} \leq B_{\tilde{\kappa}}\,, \tag{51}$$

and the corresponding upper bounds for the components κ_v and $\boldsymbol{\kappa}_\omega$, which we denote by B_κ^v, $B_{\tilde{\kappa}}^v$, B_κ^ω and $B_{\tilde{\kappa}}^\omega$.

Properties of $\mathbf{C}(s)$ and $\hat{\mathbf{C}}(s)$:
We select $d_v(s)$ in (14) such that $\mathbf{C}_v(s)$ and $\hat{\mathbf{C}}_v(s)$ are fourth order low-pass filters with DC gains equals $\mathbf{I}_{3\times3}$ and we select $\mathbf{d}_\omega(s)$ in (33) such that $\mathbf{C}_\omega(s)$ and $\hat{\mathbf{C}}_\omega(s)$ are first order low-pass filters with DC gains also equals $\mathbf{I}_{3\times3}$. We further need to ensure that $\forall\boldsymbol{\kappa} \in \mathbb{K}$ the aforementioned filters and in addition $s\mathbf{C}_v(s)$, $s^2\mathbf{C}_v(s)$ and $s^3\mathbf{C}_v(s)$ are strictly proper and exponentially stable.

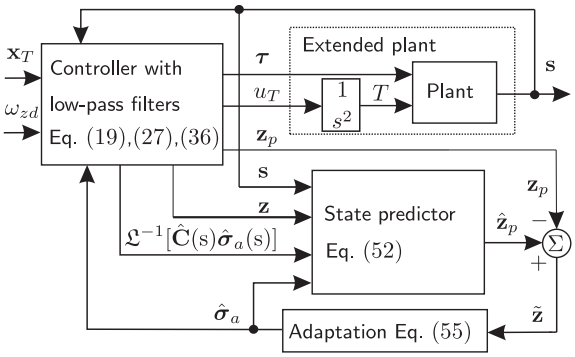

Figure 1: Closed-loop system with the desired position trajectory $\mathbf{x}_T$ and the desired angular rate ω_{zd}. The values contained in $\mathbf{s} = \{\mathbf{x}, \boldsymbol{v}, \dot{\boldsymbol{v}}, \mathbf{R}, \boldsymbol{\omega}, T, \dot{T}\}$ are measurements required for control.

In the following, we first define a state predictor and an adaptation law to estimate the uncertainties. Then, we introduce a reference model, which represents the behavior of our error system (43) with perfect adaptation inside the chosen frequency range. For this system, we provide a sufficient stability condition and bounds for its control inputs. With the knowledge of the maximal estimation error, we can then state sufficient stability conditions for the closed-loop system and bounds of the control signals. The closed-loop system is shown in Fig. 1. The reference model solely serves for analysis and is not implemented in the controller.

3.3 State predictor

Since not all states are directly affected by the uncertainties in $\boldsymbol{\sigma}_a = [\boldsymbol{\sigma}_{va}', \boldsymbol{\sigma}_{\omega a}']'$, it is sufficient to consider the states $\mathbf{z}_v$, $z_{\omega z}$ and the first two entries of $\mathbf{z}_r$, denoted by $\mathbf{z}_{r12}$, for the state predictor. The remaining states can be replaced by their measured values. Hence our state predictor is a reduced version of the error dynamics in (43) and takes the form

$$\dot{\hat{\mathbf{z}}}_p = \underbrace{\begin{bmatrix} -\mathbf{z}_x + \mathbf{A}_v\hat{\mathbf{z}}_v + \hat{\kappa}_v\mathbf{z}_t \\ -\mathbf{M}_{12}'\mathbf{z}_t + \mathbf{A}_{r12}\hat{\mathbf{z}}_{r12} \\ a_{\omega z}\hat{z}_{\omega z} \end{bmatrix}}_{:=\hat{\mathbf{f}}(t,\hat{\mathbf{z}}_p,\mathbf{z},\hat{\boldsymbol{\eta}}_{in})} + \hat{\boldsymbol{\sigma}}_a - \mathfrak{L}^{-1}[\hat{\mathbf{C}}(s)\hat{\boldsymbol{\sigma}}_a(s)]\,, \tag{52}$$

- 10.1515/auto-2013-1035

with the predictor states $\hat{\mathbf{z}}_p := [\hat{\mathbf{z}}_v', \hat{\mathbf{z}}_{r12}', \hat{z}_{\omega z}]'$ and with $\mathbf{M}_{12}'$ and $\mathbf{A}_{r12}$ being the corresponding submatrices of $\mathbf{M}'$ and $\mathbf{A}_r$ respectively.

3.4 Estimation error dynamics

The estimation error is defined as $\tilde{\mathbf{z}} = \hat{\mathbf{z}}_p - \mathbf{z}_p$, where $\mathbf{z}_p := [\mathbf{z}_v', \mathbf{z}_{r12}', z_{\omega z}]'$ holds. The dynamics for $\mathbf{z}_p$ result from (43), with (16) and (31), and read

$$\dot{\mathbf{z}}_p = \hat{\mathbf{f}}(t, \mathbf{z}_p, \mathbf{z}, \hat{\boldsymbol{\eta}}_{va}) + \boldsymbol{\sigma}_a - \mathfrak{L}^{-1}[\hat{\mathbf{C}}_a(s)\hat{\boldsymbol{\sigma}}_a(s)] - \tilde{\boldsymbol{\kappa}}\mathbf{u}_a - \tilde{\boldsymbol{\kappa}}\mathbf{u}_n . \tag{53}$$

The estimation error dynamics arise from a subtraction of (53) from (52) and is given by

$$\dot{\tilde{\mathbf{z}}} = \mathbf{A}_e\tilde{\mathbf{z}} + \tilde{\boldsymbol{\sigma}}_a + \tilde{\boldsymbol{\kappa}}\mathbf{u}_a + \tilde{\boldsymbol{\kappa}}\mathbf{u}_n , \tag{54}$$

where $\mathbf{A}_e = \mathrm{diag}(\mathbf{A}_v, \mathbf{A}_{r12}, a_{\omega z})$ and $\tilde{\mathbf{z}}(t=0) = 0$.

3.5 Adaptation law

We use the Piecewise-Constant Adaptation Law from [10, 11], which is defined for our application as

$$\hat{\boldsymbol{\sigma}}_a = \hat{\boldsymbol{\sigma}}_a(iT_s) , \quad t \in [iT_s, (i+1)T_s) , \tag{55}$$

$$\hat{\boldsymbol{\sigma}}_a(iT_s) = -\boldsymbol{\Phi}^{-1}(T_s)\boldsymbol{\mu}(iT_s) , \tag{56}$$

with $i \in \mathbb{N}_0$ and the adaptation sampling time T_s, where

$$\boldsymbol{\Phi}(T_s) = \mathbf{A}_e^{-1}(\mathbf{e}^{\mathbf{A}_e T_s} - \mathbf{I}) \tag{57}$$

$$\boldsymbol{\mu}(iT_s) = \mathbf{e}^{\mathbf{A}_e T_s}\tilde{\mathbf{z}}(iT_s) . \tag{58}$$

To adjust the adaptation speed, we reduce or increase the sampling time T_s, which can be arbitrary small with sufficient CPU power. At least it must be chosen small enough to verify a certain performance condition given by (80) in the subsequent Section 3.7. Due to limited space, we refer the interested reader to the references for more insight into this adaptation concept.

3.6 Reference model

The reference model arises from (43) with the best estimation result achievable for our control structure, i.e. $\hat{\boldsymbol{\sigma}}_{a,\mathrm{ref}} = \boldsymbol{\sigma}_{a,\mathrm{ref}} - \tilde{\boldsymbol{\kappa}}\mathbf{u}_{a,\mathrm{ref}} - \tilde{\boldsymbol{\kappa}}\mathbf{u}_{n,\mathrm{ref}}$, see (54). Hence the reference model has the structure

$$\dot{\mathbf{z}}_{\mathrm{ref}} = \mathbf{f}(t, \mathbf{z}_{\mathrm{ref}}, \boldsymbol{\eta}_{va,\mathrm{ref}}) + \mathbf{B}(\boldsymbol{\sigma}_{a,\mathrm{ref}} - \boldsymbol{\eta}_{a,\mathrm{ref}} - \tilde{\boldsymbol{\kappa}}\mathbf{u}_{n,\mathrm{ref}}) , \tag{59}$$

with $\mathbf{z}_{\mathrm{ref}}(0) = \mathbf{z}_0$ and

$$\boldsymbol{\eta}_{a,\mathrm{ref}}(s) = \mathbf{C}(s)(\boldsymbol{\sigma}_{a,\mathrm{ref}}(s) - \tilde{\boldsymbol{\kappa}}\mathbf{u}_{n,\mathrm{ref}}(s)) , \tag{60}$$

$$[\mathbf{T}_{d,\mathrm{ref}}' \; \boldsymbol{\tau}_{\mathrm{ref}}']' = -\hat{\boldsymbol{\kappa}}^{-1}\boldsymbol{\sigma}_{n,\mathrm{ref}} - \boldsymbol{\kappa}^{-1}\boldsymbol{\eta}_{a,\mathrm{ref}} . \tag{61}$$

Even though we decoupled the nominal control signals from the adaptation, we are able to compensate for the influence of the uncertain input gains in the frequency range where $\mathbf{C}(s) \approx \mathbf{I}_{6\times 6}$ holds.

Properties of $\mathbf{f}$, $\hat{\boldsymbol{\eta}}_{va}$, $\boldsymbol{\sigma}_{kl}$ and $\dot{\boldsymbol{\sigma}}_{kl}$, $k \in \{v, \omega\}$, $l \in \{a, n\}$: All ten functions, given in (12), (13), (17), (30) and (43), depend on the desired trajectory, the model uncertainties, the error states and the adaption error. Since first, we track a sufficiently smooth and bounded trajectory, more precisely we choose $\mathbf{x}_T \in C^5$, and second, assume $T \geq T_{\min} > 0$, see Remark 2, and third, assume (2) and (5) to be differentiable in their arguments and bounded, these ten functions are differentiable in their arguments and bounded in $t \in \mathbb{R}_0^+$. Thus we can find the following bound regarding the initialization

$$\left\|\boldsymbol{\sigma}_{kl}|_{t=0}\right\| \leq B_{\sigma 0}^{kl} \tag{62}$$

and $\forall t$ and $\forall \mathbf{z} \in \mathcal{Z}$, $\forall \mathbf{z}_{\mathrm{ref}} \in \mathcal{Z}_{\mathrm{ref}}$, $\forall \tilde{\mathbf{z}} \leq \bar{\gamma}_0$ the constants L_{σ}^{kl}, B_{σ}^{kl}, $L_{\dot{\sigma}}^{kl}$, $B_{\dot{\sigma}}^{kl}$, L_{η}^{ka} and B_{η}^{ka} exist such that

$$\left\|\boldsymbol{\sigma}_{kl} - \boldsymbol{\sigma}_{kl,\mathrm{ref}}\right\| \leq L_{\sigma}^{kl}\gamma , \tag{63}$$

$$\left\|\boldsymbol{\sigma}_{kl,\mathrm{ref}}\right\| \leq B_{\sigma}^{kl} , \tag{64}$$

$$\left\|\dot{\boldsymbol{\sigma}}_{kl} - \dot{\boldsymbol{\sigma}}_{kl,\mathrm{ref}}\right\| \leq L_{\dot{\sigma}}^{kl}\gamma , \tag{65}$$

$$\left\|\dot{\boldsymbol{\sigma}}_{kl,\mathrm{ref}}\right\| \leq B_{\dot{\sigma}}^{kl} , \tag{66}$$

$$\left\|\hat{\boldsymbol{\eta}}_{ka} - \boldsymbol{\eta}_{ka,\mathrm{ref}}\right\| \leq L_{\eta}^{ka}\gamma , \tag{67}$$

$$\left\|\boldsymbol{\eta}_{ka,\mathrm{ref}}\right\| \leq B_{\eta}^{ka} . \tag{68}$$

Further, since the gradient of $\mathbf{f}$ with respect to $\mathbf{z}_\eta := [\mathbf{z}', \hat{\boldsymbol{\eta}}_{va}']'$, denoted as $\partial_z\mathbf{f}$, is also differentiable in its arguments, we can find a constant $L_{\partial\mathbf{f}}$ such that

$$\left\|\partial_z\mathbf{f} - \partial_z\mathbf{f}_{\mathrm{ref}}\right\| \leq L_{\partial\mathbf{f}}\left\|\mathbf{z}_\eta - \mathbf{z}_{\eta,\mathrm{ref}}\right\| \leq L_{\partial\mathbf{f}}(1 + L_{\eta}^{va})\gamma . \tag{69}$$

With this properties we can state the following:

Lemma 1. For the reference system in (59), with the strictly proper and exponentially stable transfer function $\mathbf{G}_k(s)$, defined as $\mathbf{G}_k(s) := s^{-1}(\mathbf{I}_{3\times 3} - \mathbf{C}_k(s))$, $k \in \{v, \omega\}$, if $d_v(s)$ and $\mathbf{d}_\omega(s)$ in (14) and (33) are chosen such that

$$\rho_{\mathrm{ref}} > \sqrt{\left\|\mathbf{z}_0\right\|^2 + 2\,r(\left\|\mathbf{G}_k(s)\right\|_{\mathcal{L}_1})}, \quad k \in \{v, \omega\} \tag{70}$$

holds, where $r(\|\mathbf{G}_k(s)\|_{\mathcal{L}_1}) =$ (71)

$$\frac{\rho_{\text{ref}}}{2\sigma_{\text{m}}}\sum_{k=v}^{\omega}\|\mathbf{B}_k\|\,\|\mathbf{G}_k(s)\|_{\mathcal{L}_1}\left(B_{\sigma 0}^{ka}+B_{\tilde{\kappa}}^{k}B_{\sigma 0}^{kn}+B_{\dot{\sigma}}^{ka}+B_{\tilde{\kappa}}^{k}B_{\dot{\sigma}}^{kn}\right),$$

with $\mathbf{B}_k$ from (41) and (42) and with σ_{m} being the minimal singular value of $\mathbf{A}_V$ in (40), then $\forall t \geq 0$

$$\|\mathbf{z}_{\text{ref}}\| < \rho_{\text{ref}} \quad \leftrightarrow \quad \mathbf{z}_{\text{ref}} \in \text{Int}\{\mathcal{Z}_{\text{ref}}\}, \tag{72}$$

$$\|\mathbf{T}_{d,\text{ref}}\| \leq \hat{\kappa}_v^{-1}B_{\sigma}^{vn} + B_{\kappa}^{v}B_{\eta}^{va} =: \rho_{\text{Tref}}, \tag{73}$$

$$\|\boldsymbol{\tau}_{\text{ref}}\| \leq \|\hat{\boldsymbol{\kappa}}_{\omega}^{-1}\|\,B_{\sigma}^{\omega n} + B_{\kappa}^{\omega}B_{\eta}^{\omega a} =: \rho_{\boldsymbol{\tau}\text{ref}}\,. \tag{74}$$

The proof of Lemma 1 is given in the appendix.

Remark 3. Since $\mathbf{C}_k(s)$, $k \in \{v, \omega\}$ is chosen to be strictly proper and exponentially stable with DC gain equals $\mathbf{I}_{3\times 3}$, see Sec. 3.2, we know that the transfer function $\mathbf{G}_k(s) = s^{-1}(\mathbf{I}_{3\times 3} - \mathbf{C}_k(s))$ is also strictly proper and exponentially stable since $\mathbf{I}_{3\times 3} - \mathbf{C}_k(s)$ has a zero in the origin that cancels the pole s^{-1}.

Remark 4. The reference control input for the extended plant model $u_{T,\text{ref}}$, which is included in (59), is a continuous function of $\mathbf{z}_{\text{ref}}$ and t. Since we have $\mathbf{z}_{\text{ref}} \in \mathcal{Z}_{\text{ref}}$ and since we chose a bounded trajectory $\mathbf{x}_T \in C^5$, see (27), we know that $u_{T,\text{ref}}$ is also bounded. But because of limited space, we do not derive this bound.

Remark 5. In order to fulfill condition (70) for a given $\mathbf{z}_0$ and ρ_{ref}, one can use $d_v(s)$ and $\mathbf{d}_{\omega}(s)$ to increase or decrease the bandwidth of $\mathbf{C}_k(s)$. An increase, i.e. $\mathbf{C}_k(s) \to \mathbf{I}_{3\times 3}$, yield faster dynamics of $\mathbf{G}_k(s)$ and lowers the value for $\|\mathbf{G}_k(s)\|_{\mathcal{L}_1}$. To illustrate this relation, we may think of the case $\mathbf{C}_k(s) = \Omega(s+\Omega)^{-1}\mathbf{I}_{3\times 3}$, which yields $\|\mathbf{G}_k(s)\|_{\mathcal{L}_1} \leq \|(s+\Omega)^{-1}\mathbf{I}_{3\times 3}\|_{\mathcal{L}_1} = \Omega^{-1}$. In addition, we can also increase the controller gains in $\mathbf{A}_V$, leading to higher values for σ_{m}. On the contrary, one may choose a higher value for ρ_{ref} and realize a lower filter bandwidth of $\mathbf{C}_k(s)$ and lower controller gains in $\mathbf{A}_V$. The latter choice yields lower performance but higher robustness in comparison to the former.

3.7 Transient and Steady-State Performance

The following sufficient conditions ensure a bounded and stable tracking performance of the complete closed-loop system:

First condition: With $k(t)$ defined as

$$k(t) := 2L_{\partial \text{f}}(1 + L_{\eta}^{va})\gamma + L_{\partial \text{f}}(\varepsilon(t) + B_{\eta}^{va}), \text{ where} \tag{75}$$

$$\varepsilon(t) := \sqrt{e^{-2\sigma_{\text{m}}t}\|\mathbf{z}_0\|^2 + 2\,r(\|\mathbf{G}_k(s)\|_{\mathcal{L}_1})}\,, \tag{76}$$

and with the convergence time $t = T$, we must verify

$$\sigma_{\text{m}} > k(T)\,, \tag{77}$$

where σ_{m} is the minimal singular value of $\mathbf{A}_V$ in (40) and T can be freely chosen. $\varepsilon(t)$ is a time varying upper bound for $\|\mathbf{z}_{\text{ref}}\|$.

This condition restricts the difference of the real system from the reference system such that the Lyapunov function for the nominal system, i.e $V(\mathbf{z})$ in (38), can be used to analyze the dynamics for $\mathbf{e} := \mathbf{z} - \mathbf{z}_{\text{ref}}$ obtained by a subtraction of (59) from (43).

Second condition: We must further fulfill (78)

$$c_1 := \frac{2\xi}{|\bar{\lambda}|}\left(\bar{k}L_{\eta}^{va} + \sum_{k=v}^{\omega}\|\mathbf{B}_k\|\|\mathbf{G}_k(s)\|_{\mathcal{L}_1}(L_{\dot{\sigma}\gamma}^{ka} + B_{\tilde{\kappa}}^{k}L_{\dot{\sigma}\gamma}^{kn})\right) \overset{!}{<} 1,$$

with $\xi := \exp(2L_{\partial \text{f}}\rho_{\text{ref}}T)$, $\bar{\lambda} := 2k(T) - 2\sigma_{\text{m}}$ and $\bar{k} = k(0)$. In addition, the arbitrary value g_0 defined in (50) has to verify

$$g_0 \leq \frac{1-c_1}{c_0}, \quad \text{with } c_0 := \frac{2\xi}{|\bar{\lambda}|}\,\|\mathbf{B}\|\,B_{\text{CHe}}\,, \tag{79}$$

where $B_{\text{CHe}} \geq \|\mathbf{C}(s)\mathbf{H}_e^{-1}(s)\|_{\mathcal{L}_1}$ and $\mathbf{H}_e^{-1}(s) := s\mathbf{I} - \mathbf{A}_e$.

The second condition ensures that the probably destabilizing uncertainties grow slower with $\mathbf{e}$ than the stabilizing terms. Hence this condition ensures a positive invariant set around the equilibrium $\mathbf{z} = \mathbf{0}$.

Third condition: The adaptation sampling time T_s must be chosen such that

$$\gamma_0(T_s) < g_0\gamma = \bar{\gamma}_0\,, \tag{80}$$

where $\gamma_0(T_s)$ is defined in [10, Ch. 3.3.] for a general case that covers our application. Hence we refer the interested reader to the given reference. Lemma 3.3.1 in [10] provides that $\lim_{T_s \to 0}\gamma_0(T_s) = 0$ holds.

The third condition limits the maximum estimation error such that the positive invariant set around the equilibrium $\mathbf{z} = \mathbf{0}$ is contained inside the set $\mathcal{Z}$ defined in (49).

To assess the maximum estimation error, we can apply Lemma 3.3.3 in [10], which suits our application with minor changes, involving the use of the Euclidean norm instead of the infinity norm. This Lemma formulated for our application reads:

Lemma 2. If (70), (77), (78) and (80) are satisfied and further $\|\mathbf{z}\| \leq \rho$ holds $\forall t \in [0, \tau]$, we have

$$\|\tilde{\mathbf{z}}\| < \bar{\gamma}_0\,, \quad \forall t \in [0, \tau]\,. \tag{81}$$

The proof is very similar to that given in [10, Ch. 3.3.] and therefore omitted.

The existence of the bound ρ has not been ensured so far, but this is part of the following final result:

Theorem 1 (Main result). Given the error system (43) and the reference system (59), provided condition (70), (77) and (78) hold and let the adaptation rate be chosen to satisfy (80), we have $\forall t \geq 0$, with $\mathbf{e} := \mathbf{z} - \mathbf{z}_{\text{ref}}$,

$$\|\mathbf{z}\| < \rho \quad \leftrightarrow \quad \mathbf{z} \in \text{Int}(\mathcal{Z}), \tag{82}$$
$$\|\mathbf{T}_d\| \leq \rho_{\text{T}}, \tag{83}$$
$$\|\boldsymbol{\tau}\| \leq \rho_{\boldsymbol{\tau}}, \tag{84}$$
$$\|\tilde{\mathbf{z}}\| < \bar{\gamma}_0, \tag{85}$$
$$\|\mathbf{e}\| < \gamma, \tag{86}$$

where

$$\rho_{\text{T}} := \hat{\kappa}_v^{-1}(B_\sigma^{vn} + L_\sigma^{vn}\gamma) + B_\kappa^v(B_\eta^{va} + L_\eta^{va}\gamma), \tag{87}$$
$$\rho_{\boldsymbol{\tau}} := \left\|\hat{\boldsymbol{\kappa}}_\omega^{-1}\right\|(B_\sigma^{\omega n} + L_\sigma^{\omega n}\gamma) + B_\kappa^\omega(B_\eta^{\omega a} + L_\eta^{\omega a}\gamma). \tag{88}$$

The proof is given in the appendix.

Remark 6. The bounds given in Theorem 1 imply the boundedness of the input signal u_T, see Remark 4. Due to limited space we do not derive this bound.

4 Simulation and experimental results

We analyzed the presented controller in simulations, as well as in experimental tests. For the simulations, we implemented the plant model from Sec. 2 and designed the adaptive controller accordingly to the uncertainties and time-varying disturbances given in Table 1. We used $d_v(s)$ and $\mathbf{d}_\omega(s)$ to place the eigenvalues of $\hat{\mathbf{C}}(s)$ such that $\hat{f}_{v1} = -60$ Hz, $\hat{f}_{v2} = -65$ Hz, $\hat{f}_{v3} = -70$ Hz, $\hat{f}_{v4} = -80$ Hz held for $\hat{\mathbf{C}}_v(s)$ and $\hat{f}_\omega = -32$ Hz for $\hat{\mathbf{C}}_\omega(s)$. With the chosen control parameters, trajectory characteristics, uncertainty ranges

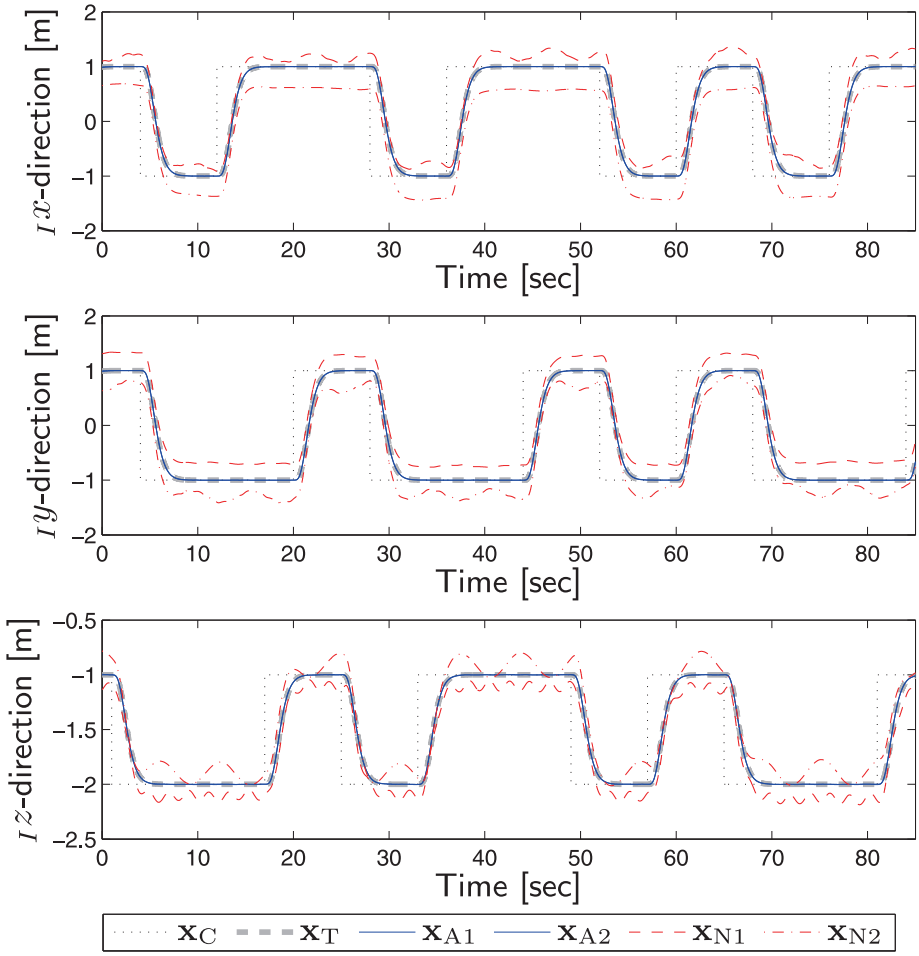

Figure 2: Simulation results verifying the transition between the set points $\mathbf{x}_C$ along the desired trajectory $\mathbf{x}_T$ of the presented adaptive controller $\mathbf{x}_{A1}/\mathbf{x}_{A2}$ and the nonadaptive version $\mathbf{x}_{N1}/\mathbf{x}_{N2}$. The plant was affected by the uncertainties given in Table 2 indicated by the indices $_1$ and $_2$ respectively. Note that we used the same line style for $\mathbf{x}_{A1}$ and $\mathbf{x}_{A2}$, because the adaptive controller performed very similar for each case.

and design variables and bounds, all given in Table 1, we obtained $\|\mathbf{G}_v(s)\|_{\mathcal{L}_1} < 0.016$ and $\|\mathbf{G}_\omega(s)\|_{\mathcal{L}_1} < 0.0089$ and fulfilled all conditions for Theorem 1. As one may expect, the theoretically covered uncertainty ranges and the theoretically needed adaptation speed given in Table 1 are rather conservative due to the applied norm approximations. This is substantiated by our simulation results shown in Fig. 2, where we used a much wider uncertainty range, given in Table 2, and realized an adaptation sampling time of $T_s = 1$ ms. For this test, we commanded alternating set points $\mathbf{x}_C$ and provided a sufficiently smooth desired trajectory $\mathbf{x}_T \in C^5$ by ways of a linear filter. In Fig. 2 we provide the results for two differing parameter sets, both on the border of the considered uncertainty ranges. For each case we compared the adaptive controller with a nonadaptive version of the same controller to illustrate the benefit of the adaptation. The nonadaptive version was equally parametrized except that $\hat{\boldsymbol{\sigma}}_{va} = \hat{\boldsymbol{\sigma}}_{\omega a} \stackrel{!}{=} 0$ held. For the nonadaptive version, we observed huge deviations from the desired trajectory due to the uncertainties, see $\mathbf{x}_{N1}$ and $\mathbf{x}_{N2}$ in Fig. 2. For the adaptive version in turn, see $\mathbf{x}_{A1}$ and $\mathbf{x}_{A2}$ in Fig. 2, the parameter uncertainties and the time-

Table 1: Control and plant parameters used for the theoretical verification given in SI units.

Control parameters			
$\mathbf{A}_x = -2\cdot\mathbf{I}_{3\times3}$	$\mathbf{A}_v = -2\cdot\mathbf{I}_{3\times3}$	$\mathbf{A}_t = -8\cdot\mathbf{I}_{3\times3}$	
$\mathbf{A}_r = -8\cdot\mathbf{I}_{3\times3}$	$a_{\omega z} = -8$	$T_s = 10^{-7}$	
Trajectory characteristics			
$\|\mathbf{x}_T\| \le 2.4$	$\|\dot{\mathbf{x}}_T\| \le 1.6$	$\|\ddot{\mathbf{x}}_T\| \le 1.8$	
$\|\dddot{\mathbf{x}}_T\| \le 3.0$	$\|\ddddot{\mathbf{x}}_T\| \le 5.1$	$\|\overset{(5)}{\mathbf{x}}_T\| \le 18.9$	
Uncertain plant parameter ranges and disturbances			
$m \in [0.559, 0.561]$	$g \in [9.77, 9.79]$	$\kappa_v \in [1.784, 1.788]$	
$\|\mathbf{J}\| \in [3.96, 4.04]\cdot10^{-3}$	$\mathbf{f}_w = \mathbf{J}^{-1}(\mathbf{J}\boldsymbol{\omega}\times\boldsymbol{\omega})$	$\|\boldsymbol{\kappa}_\omega\| \in [396, 404]$	
$\|\mathbf{D}\| \in [0.792, 0.808]$	$\mathbf{f}_v = \mathbf{D}\boldsymbol{v}$	$\|\boldsymbol{\zeta}_v\| \le 3.8\cdot10^{-3}$	
$\|\dot{\boldsymbol{\zeta}}_v\| \le 1.0\cdot10^{-5}$	$\|\boldsymbol{\zeta}_\omega\| \le 7.4\cdot10^{-3}$	$\|\dot{\boldsymbol{\zeta}}_\omega\| \le 3.0\cdot10^{-5}$	
Adaptive design variables and bounds			
$\|\mathbf{z}_0\| \le 0.05$	$\rho_{\text{ref}} = 0.06$	$\sigma_m = 2.0$	
$r = 4.4\cdot10^{-5}$	$k(T) = 0.69$	$c_1 = 0.037$	
$c_0 = 5.1$	$\gamma = 1.0\cdot10^{-4}$	$\bar{\gamma}_0 = 1.0\cdot10^{-6}$	
$\gamma_0(T_s) = 9.0\cdot10^{-7}$	$\rho = \rho_{\text{ref}} + 1\cdot10^{-4}$	$\rho_{\text{Tref}} = 7.99$	
$\rho_T = \rho_{\text{Tref}} + 3\cdot10^{-4}$	$\rho_{\tau\text{ref}} = 0.072$	$\rho_\tau = \rho_{\tau\text{ref}} + 1\cdot10^{-6}$	
$B_{\sigma 0}^{va} = 0.011$	$B_{\sigma 0}^{vn} = 9.9$	$B_{\sigma 0}^{\omega a} = 0.022$	$B_{\sigma 0}^{\omega n} = 19.8$
$B_{\sigma}^{va} = 0.028$	$B_{\sigma}^{vn} = 14$	$B_{\sigma}^{\omega a} = 0.055$	$B_{\sigma}^{\omega n} = 28$
$L_{\sigma}^{va} = 0.021$	$L_{\sigma}^{vn} = 2.6$	$L_{\sigma}^{\omega a} = 0.051$	$L_{\sigma}^{\omega n} = 6.2$
$B_{\dot{\sigma}}^{va} = 0.020$	$B_{\dot{\sigma}}^{vn} = 6.4$	$B_{\dot{\sigma}}^{\omega a} = 0.040$	$B_{\dot{\sigma}}^{\omega n} = 13$
$L_{\dot{\sigma}}^{va} = 0.085$	$L_{\dot{\sigma}}^{vn} = 9.1$	$L_{\dot{\sigma}}^{\omega a} = 0.17$	$L_{\dot{\sigma}}^{\omega n} = 18$
$L_{\partial \mathbf{f}} = 16$	$L_{\boldsymbol{\eta}}^{va} = 0.050$	$B_{\boldsymbol{\eta}}^{va} = 0.072$	$B_{\boldsymbol{\eta}}^{\omega a} = 0.59$

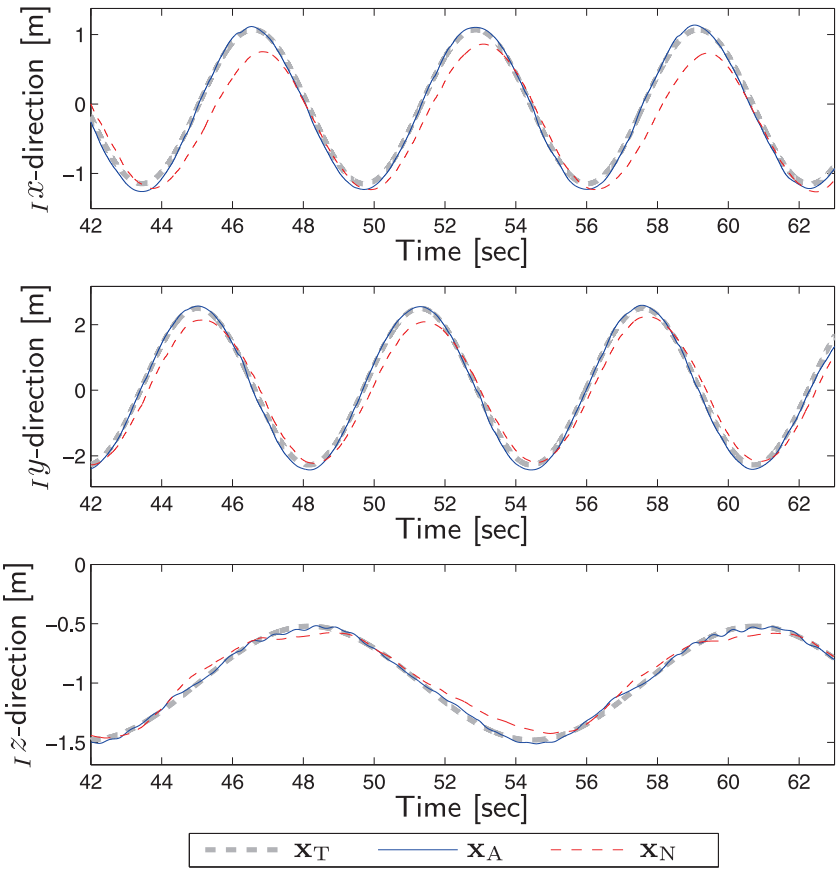

Figure 3: Experimental result verifying the tracking of a helix $\mathbf{x}_T$ for the presented adaptive controller $\mathbf{x}_A$ and the nonadaptive version $\mathbf{x}_N$.

Table 2: Plant parameters and disturbances used for simulation given in SI units. The two chosen test parameter sets are indicated by the indices$_1$ and$_2$.

Uncertain plant parameter ranges and disturbances		
$m \in [0.50_1, 0.62_2]$	$g \in [7.85_1, 11.8_2]$	$\kappa_v \in [1.43_2, 2.15_1]$
$\|\mathbf{J}\| \in [3.6_2, 4.4_1]\cdot 10^{-3}$	$\mathbf{f}_\omega = \mathbf{J}^{-1}(\mathbf{J}\boldsymbol{\omega}\times\boldsymbol{\omega})$	$\|\boldsymbol{\kappa}_\omega\| \in [320_1, 480_2]$
$\|\mathbf{D}\| \in [0.08_2, 0.12_1]$	$\mathbf{f}_v = \mathbf{D}\boldsymbol{v}$	
$\boldsymbol{\zeta}_{v1} = [2-\sin t-0.5\cdot\sin 5t+0.2\cdot\sin 10t, 3, 2+\sin 3t]'$		
$\boldsymbol{\zeta}_{v2} = -[3, 2+\sin t+0.5\cdot\sin 5t-0.2\cdot\sin 10t, 2-\sin t]'$		
$\boldsymbol{\zeta}_{\omega 1} = [2+2\cdot\sin 3t, 2+3\cdot\sin t+0.8\cdot\sin 5t-0.1\cdot\sin 20t, 2]'$		
$\boldsymbol{\zeta}_{\omega 2} = -[2, 2+3\cdot\sin t+0.8\cdot\sin 5t-0.1\cdot\sin 20t, 2+\sin 3t]'$		

varying disturbance were effectively compensated and the system tracked the desired trajectory precisely. The adaptive controller realized, $\|\boldsymbol{\tau}\| < 0.031$ and $\|\mathbf{T}_d\| < 7.7$ for all $t \geq 0$ and both parameter sets, which shows that the theoretical bounds derived for the narrow uncertainty range were met in our simulations even for the wide uncertainty range. We obtained similar results for further parameter sets inside the uncertainty ranges and disturbances below the filter frequencies of $\mathbf{C}(s)$.

Our experimental tests were performed with an AscTec Hummingbird on an indoor test rig at the Nanyang Technological University in Singapore. The test rig was equipped with a motion capturing system from Vicon and the measured position signal was sent to the quadrotor via radio link operating at 50 Hz. An on-board data fusion combined the measured position with sensor data from gyroscopes and accelerometers to provide all necessary measurement signals. The controller was running on an ARM Cortex-A8 processor at 1 kHz and required about 20 % of the available CPU power. We used the same controller parameters as given in Table 1 except the following: We reduced the filter frequencies of $\hat{\mathbf{C}}(s)$ to $\hat{f}_{v1} = -1.6$ Hz, $\hat{f}_{v2} = -1.7$ Hz, $\hat{f}_{v3} = -1.9$ Hz, $\hat{f}_{v4} = -2.1$ Hz and $\hat{f}_\omega = -1.3$ Hz since the frequencies used for simulation caused a rather poor robustness margin in the presence of measurement noise, even though we already reduced the noise level by additional filtering. Further, since a fast adaptation rate

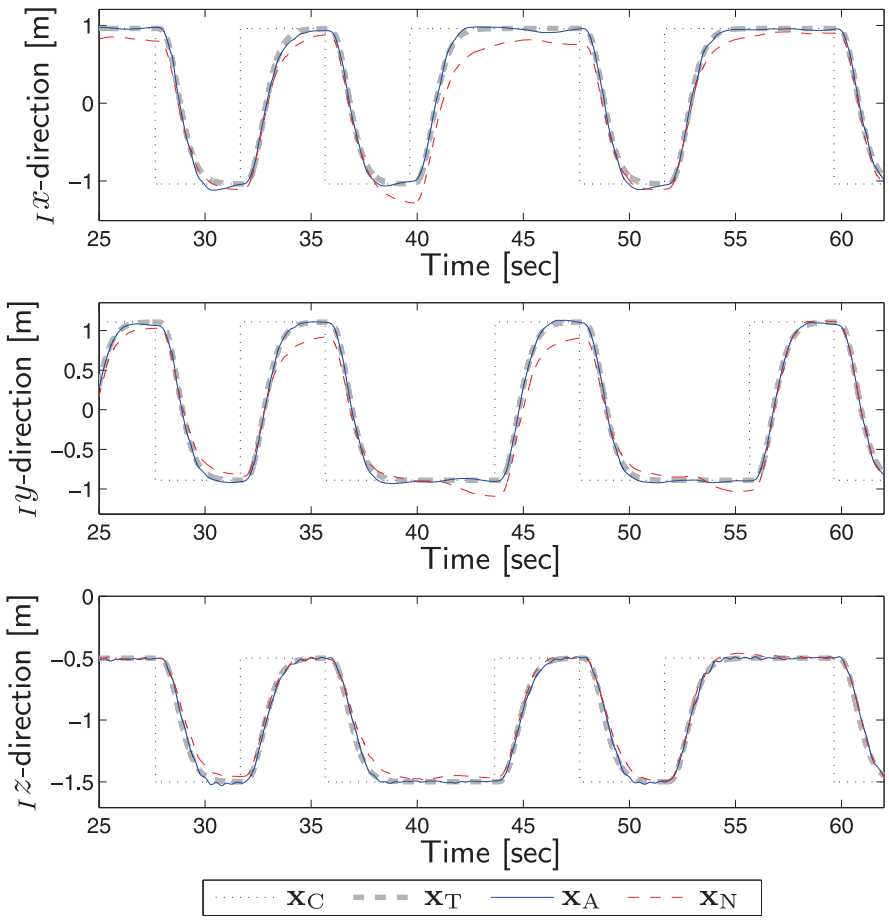

Figure 4: Experimental result verifying the transition between the set points $\mathbf{x}_C$ along the desired trajectory $\mathbf{x}_T$ for the presented adaptive controller $\mathbf{x}_A$ and the nonadaptive version $\mathbf{x}_N$.

deteriorates the above-mentioned problem concerning the noise level, we reduced the adaptation rate to 100 Hz. However we did not experimentally identify the plant parameters and nevertheless obtained fine results shown in Figs. 3 and 4 for this parameter setting. In both test cases, the adaptive controller achieved a precise tracking performance and could cancel out the uncertainties that apparently affected the nonadaptive system.

5 Conclusions

Due to the backstepping design and the chosen plant model, we realized a globally feasible and unique closed-loop behavior. We modified and extended the existing L1 adaptive control theory for nonlinear reference systems to suit our design and to preserve a maximum of maneuverability. To compensate for uncertain input parameters, the existing L1 adaptive control theory requires filtering not only the estimation signal $\hat{\boldsymbol{\sigma}}_a$, but also the nominal control signal $\boldsymbol{\sigma}_n$. However, due to the rather low chosen frequencies of $\hat{\mathbf{C}}(s)$ in our practical implementation, this additional filtering of $\boldsymbol{\sigma}_n$ would reduce the control channel bandwidth too much to obtain a stable tracking. Thus it was necessary to further modify the theory for a decoupling of the nominal control signals from the adaptation. The resulting controller turned out to be a promising solution to cope with diverse parameter uncertainties and disturbances. It may help to avoid expensive system identifications and to handle unforeseeable disturbances such as wind.

Appendix

5.1 Lemma 3

For the non-autonomous system

$$\dot{x} = \lambda\, x + \mathbf{z}'\,[\mathbf{B}_v \mathbf{B}_\omega]\,[\boldsymbol{\chi}_v' \boldsymbol{\chi}_\omega']', \qquad x(0) = 0\,, \tag{89}$$

$$\boldsymbol{\chi}_k(s) = (\mathbf{I}_{3\times 3} - \mathbf{C}_k(s))\boldsymbol{\sigma}_{kl}(s)\,, \quad k \in \{v, \omega\}\,, \tag{90}$$

where $l \in \{a, n\}$ and $\lambda < 0$ holds, $\boldsymbol{\chi}_k$ can be written as the outputs of the following system, with $k \in \{v, \omega\}$,

$$\begin{aligned}\boldsymbol{\chi}_k(s) &= \mathbf{G}_k(s)[s\boldsymbol{\sigma}_{kl}(s) - \boldsymbol{\sigma}_{kl}|_{t=0} + \boldsymbol{\sigma}_{kl}|_{t=0}] \\ &= \mathbf{G}_k(s)[\dot{\boldsymbol{\sigma}}_{kl}(s) + \boldsymbol{\sigma}_{kl}|_{t=0}]\,,\end{aligned} \tag{91}$$

with the strictly proper and exponentially stable low-pass filter $\mathbf{G}_k(s) := s^{-1}(\mathbf{I}_{3\times 3} - \mathbf{C}_k(s))$. Provided $\boldsymbol{\sigma}_{kl}|_{t=0}$ and $\dot{\boldsymbol{\sigma}}_{kl}$ are bounded for a certain time interval $t \in [0, \tau]$, such that comparable bounds as $B^{kn}_{\sigma 0}$ in (62) and $B^{kn}_{\dot{\sigma}}$ in (66) apply, than

$$\left\|\boldsymbol{\chi}_k\right\| \le \|\mathbf{G}_k(s)\|_{\mathcal{L}_1}(B^{kn}_{\dot{\sigma}} + B^{kn}_{\sigma 0})\,, \quad \forall t \in [0, \tau]\,. \tag{92}$$

Further, $x(t)$, with $t \in [0, \tau]$, is upper bounded by

$$\|x(t)\| \le \sum_{k=v}^{\omega} \int_0^t e^{\lambda(t-\nu)} \|\mathbf{z}(\nu)\| \left\|\mathbf{B}_k\right\| \left\|\boldsymbol{\chi}_k(\nu)\right\| \, d\nu \tag{93}$$

$$\le \frac{\rho}{|\lambda|} \sum_{k=v}^{\omega} \left\|\mathbf{B}_k\right\| \|\mathbf{G}_k(s)\|_{\mathcal{L}_1}(B^{kl}_{\sigma 0} + B^{kl}_{\dot{\sigma}})\,. \tag{94}$$

5.2 Proof of Lemma 1 - motivated by [20]

If the bound (72) was not true, since $\left\|\mathbf{z}_0\right\| = \left\|\mathbf{z}_{\text{ref}}(0)\right\| < \rho_{\text{ref}}$ and since $\mathbf{z}_{\text{ref}}$ is continuous, there would exist a time $\tau^* < \infty$ such that $\left\|\mathbf{z}_{\text{ref}}(t)\right\| < \rho_{\text{ref}}, \forall t \in [0, \tau^*[$ and $\left\|\mathbf{z}_{\text{ref}}(\tau^*)\right\| = \rho_{\text{ref}}$, which implies that $\left\|\mathbf{z}_{\text{ref}}\right\| \le \rho_{\text{ref}},\ \forall t \in [0, \tau^*]$. With this assumption we further know from (64) and (66) that $\forall t \in [0, \tau^*]$, $\left\|\boldsymbol{\sigma}_{kl,\text{ref}}\right\| \le B^{kl}_{\sigma}$ and $\left\|\dot{\boldsymbol{\sigma}}_{kl,\text{ref}}\right\| \le B^{kl}_{\dot{\sigma}}$ holds with $k \in \{v, \omega\}$, $l \in \{a, n\}$. With this knowledge we apply the Lyapunov candidate function in (38) for our reference system in (59), i.e. $V_{\text{ref}} = V(\mathbf{z}_{\text{ref}}) = \frac{1}{2}\,\mathbf{z}'_{\text{ref}}\,\mathbf{z}_{\text{ref}}$, and obtain for its derivative, with σ_{m} being the minimal singular value of $\mathbf{A}_V$ in (40),

$$\begin{aligned}\dot{V}_{\text{ref}} &\le -\sigma_{\text{m}} \left\|\mathbf{z}_{\text{ref}}\right\|^2 + \mathbf{z}'_{\text{ref}}\,\mathbf{B}(\boldsymbol{\sigma}_{a,\text{ref}} - \boldsymbol{\eta}_{a,\text{ref}} - \tilde{\boldsymbol{\kappa}}\mathbf{u}_{n,\text{ref}}) \\ &= -2\sigma_{\text{m}} V_{\text{ref}} + \mathbf{z}'_{\text{ref}}\,\mathbf{B}(\boldsymbol{\sigma}_{a,\text{ref}} - \boldsymbol{\eta}_{a,\text{ref}} - \tilde{\boldsymbol{\kappa}}\mathbf{u}_{n,\text{ref}}).\end{aligned} \tag{95}$$

All estimations and bounds in the following hold $\forall t \in [0, \tau^*]$. With (95), we obtain

$$V_{\text{ref}} \le \phi(t) \cdot V_{\text{ref}}(\mathbf{z}_0) + V_r\,, \tag{96}$$

where $\phi(t) := e^{-2\sigma_{\text{m}} t}$ and

$$V_r := \int_0^t \phi(t-\tau)\mathbf{z}'_{\text{ref}}\mathbf{B}(\boldsymbol{\sigma}_{a,\text{ref}} - \boldsymbol{\eta}_{a,\text{ref}} - \tilde{\boldsymbol{\kappa}}\mathbf{u}_{n,\text{ref}})d\tau\,.$$

Using (60), one can verify that V_r is the solution for

$$\begin{aligned}&\dot{V}_r = -2\sigma_{\text{m}} V_r + \mathbf{z}'_{\text{ref}}[\mathbf{B}_v \mathbf{B}_\omega]\,[\boldsymbol{\chi}_v' \boldsymbol{\chi}_\omega']'\,,\ V_r(0) = 0\,, \\ &\boldsymbol{\chi}_k(s) = (\mathbf{I}_{3\times 3} - \mathbf{C}_k(s))\mathfrak{L}[\boldsymbol{\sigma}_{ka,\text{ref}} + \tilde{\boldsymbol{\kappa}}_k \hat{\boldsymbol{\kappa}}_k^{-1}\boldsymbol{\sigma}_{kn,\text{ref}}]\,,\end{aligned} \tag{97}$$

where $k \in \{v, \omega\}$. With Lemma 3 and the definition of $r(\|\mathbf{G}_k(s)\|_{\mathcal{L}_1})$ in (71), we obtain $\left\|V_r\right\| \le r(\|\mathbf{G}_k(s)\|_{\mathcal{L}_1})$ and

$$V_{\text{ref}} \le e^{-2\sigma_{\text{m}} t}\, V_{\text{ref}}(\mathbf{z}_0) + r(\|\mathbf{G}_k(s)\|_{\mathcal{L}_1})\,. \tag{98}$$

$\mathbf{z}_{\text{ref}}$ is consequently upper bounded by

$$\|\mathbf{z}_{\text{ref}}\| \leq \sqrt{\|\mathbf{z}_0\|^2 + 2r(\|\mathbf{G}_k(s)\|_{\mathcal{L}_1})} \tag{99}$$

and with condition (70) we know that

$$\|\mathbf{z}_{\text{ref}}\| < \rho_{\text{ref}}\,, \tag{100}$$

which contradicts the assumption $\|\mathbf{z}_{\text{ref}}(\tau^\star)\| = \rho_{\text{ref}}$ and proves (72). Since $\mathbf{z}_{\text{ref}} \in \mathcal{Z}_{\text{ref}}$, $\forall t \geq 0$, the bounds on $\mathbf{T}_{d,\text{ref}}$ and $\boldsymbol{\tau}_{\text{ref}}$ in (73) and (74) follow directly from (61).

5.3 Proof of Theorem 1 - motivated by [20]

Assume the bound (86) was not true. Then, since $\|\mathbf{e}(0)\| = 0 < \gamma$ holds and since $\mathbf{e}$ is continuous, there would exist a τ such that $\|\mathbf{e}(\tau)\| = \gamma$, while $\forall t \in [0, \tau[$, $\|\mathbf{e}(t)\| < \gamma$ holds. That implies that $\forall t \in [0, \tau]$ the following inequality would hold:

$$\|\mathbf{e}\| \leq \gamma\,. \tag{101}$$

Assumed condition (70) is fulfilled, we have $\forall t \geq 0$, $\|\mathbf{z}_{\text{ref}}\| < \rho_{\text{ref}}$ and it follows that $\forall t \in [0, \tau]$,

$$\|\mathbf{z}\| < \rho_{\text{ref}} + \gamma = \rho\,. \tag{102}$$

In order to show that this result holds $\forall t \geq 0$, we analyze the difference of (43) and (59), which reads with $\mathbf{e}_\eta = \mathbf{z}_\eta - \mathbf{z}_{\eta,\text{ref}} = [\mathbf{e}', \boldsymbol{\eta}'_{va,e}]'$, where $\mathbf{z}_\eta := [\mathbf{z}', \hat{\boldsymbol{\eta}}'_{va}]'$ and $\mathbf{z}_{\eta,\text{ref}} := [\mathbf{z}'_{\text{ref}}, \boldsymbol{\eta}'_{va,\text{ref}}]'$,

$$\dot{\mathbf{e}} = \mathbf{f}(t, \mathbf{e}_\eta) + \Delta\mathbf{f}(t, \mathbf{e}_\eta, \mathbf{z}_{\eta,\text{ref}}) + \mathbf{B}(\boldsymbol{\phi}_1 + \boldsymbol{\phi}_2 + \boldsymbol{\phi}_3)\,, \tag{103}$$

where

$$\begin{aligned}
\Delta\mathbf{f}(t, \mathbf{e}_\eta, \mathbf{z}_{\eta,\text{ref}}) &= \mathbf{f}(t, \mathbf{z}_{\eta,\text{ref}} + \mathbf{e}_\eta) - \mathbf{f}(t, \mathbf{z}_{\eta,\text{ref}}) - \mathbf{f}(t, \mathbf{e}_\eta)\,,\\
\boldsymbol{\phi}_1(s) &= -\mathbf{C}(s)(\tilde{\boldsymbol{\sigma}}_a(s) + \tilde{\boldsymbol{\kappa}}\mathbf{u}_a(s) + \tilde{\boldsymbol{\kappa}}\mathbf{u}_n(s))\,,\\
\boldsymbol{\phi}_2(s) &= (\mathbf{I}_{6\times 6} - \mathbf{C}(s))\tilde{\boldsymbol{\kappa}}\hat{\boldsymbol{\kappa}}^{-1}(\boldsymbol{\sigma}_n(s) - \boldsymbol{\sigma}_{n,\text{ref}}(s))\,,\\
\boldsymbol{\phi}_3(s) &= (\mathbf{I}_{6\times 6} - \mathbf{C}(s))(\boldsymbol{\sigma}_a(s) - \boldsymbol{\sigma}_{a,\text{ref}}(s))\,.
\end{aligned}$$

The estimation error dynamics in (54) yield

$$\begin{aligned}
&\mathbf{C}(s)(\tilde{\boldsymbol{\sigma}}(s) + \tilde{\boldsymbol{\kappa}}\mathbf{u}_a(s) + \tilde{\boldsymbol{\kappa}}\mathbf{u}_n(s))\\
&= \mathbf{C}(s)(s\mathbf{I} - \mathbf{A}_e)\tilde{\mathbf{z}}(s) = \mathbf{C}(s)\mathbf{H}_e^{-1}(s)\tilde{\mathbf{z}}(s)
\end{aligned} \tag{104}$$

and further since $\mathbf{f}(t, \mathbf{z}_\eta{=}\mathbf{0}){=}\mathbf{0}$, we can write $\Delta\mathbf{f}(t, \mathbf{e}_\eta, \mathbf{z}_{\eta,\text{ref}})$ with $0 < \lambda_j < 1$, $j \in \{1, 2\}$ as

$$\Delta\mathbf{f} = \left(\int_0^1 \frac{\partial\mathbf{f}}{\partial\mathbf{z}_\eta}(t, \lambda_1\mathbf{e}_\eta + \mathbf{z}_{\eta,\text{ref}})d\lambda_1 - \int_0^1 \frac{\partial\mathbf{f}}{\partial\mathbf{z}_\eta}(t, \lambda_2\mathbf{e}_\eta)d\lambda_2\right)\mathbf{e}_\eta\,. \tag{105}$$

All estimations and bounds in the following are considered to hold $\forall t \in [0, \tau]$. Since $\mathbf{z}_{\text{ref}} \in \mathcal{Z}_{\text{ref}}$ and $\mathbf{z} \in \mathcal{Z}$ hold for this period, Lemma 2 yields $\|\tilde{\mathbf{z}}\| \leq \bar{\gamma}_0$. Further the bounds (63) - (69) hold and we obtain for (105):

$$\begin{aligned}
\|\Delta\mathbf{f}\| &\leq 2L_{\partial\mathbf{f}}\|\mathbf{e}_\eta\|^2 + L_{\partial\mathbf{f}}\|\mathbf{z}_{\eta,\text{ref}}\|\|\mathbf{e}_\eta\| && (106)\\
&< k(t)\,(\|\mathbf{e}\| + L_\eta^{va}\gamma)\,, && (107)
\end{aligned}$$

where $k(t)$ is defined in (75). Next we apply the Lyapunov candidate function in (38) to the error system in (103), i.e. $V_e = V(\mathbf{e}) = \frac{1}{2}\mathbf{e}'\mathbf{e}$, and obtain for its derivative, $\bar{k} = k(0)$ and B_{CHe} defined in (79),

$$\begin{aligned}
&\dot{V}_e \leq -2\sigma_{\text{m}}V_e + \mathbf{e}'(\Delta\mathbf{f} + \mathbf{B}(\boldsymbol{\phi}_1 + \boldsymbol{\phi}_2 + \boldsymbol{\phi}_3)) \leq\\
&-2(\sigma_{\text{m}} - k(t))V_e + \gamma^2\bar{k}L_\eta^{va} + \gamma\|\mathbf{B}\|B_{\text{CHe}}\bar{\gamma}_0 + \mathbf{e}'\mathbf{B}(\boldsymbol{\phi}_2 + \boldsymbol{\phi}_3)\,.
\end{aligned}$$

Since $\mathbf{e}(0) = 0$ we can write

$$V_e \leq \int_0^t \varphi(t, \nu)\left(\gamma^2\bar{k}L_\eta^{va} + \gamma\|\mathbf{B}\|B_{\text{CHe}}\bar{\gamma}_0 + \mathbf{e}'\mathbf{B}(\boldsymbol{\phi}_2 + \boldsymbol{\phi}_3)\right)d\nu,$$

$$\text{with}\quad \varphi(t, \nu) := \exp\left(-2\sigma_{\text{m}}(t - \nu) + 2\int_\nu^t k(\lambda)d\lambda\right),$$

which is upper bounded by: $\varphi(t, \nu) <$

$$\begin{aligned}
&< \exp\Big(-2\sigma_{\text{m}}(t-\nu) + 4L_{\partial\mathbf{f}}(1 + L_\eta^{va})\gamma(t-\nu) && (108)\\
&\qquad + 2L_{\partial\mathbf{f}}B_\eta^{va}(t-\nu) + 2L_{\partial\mathbf{f}}\int_\nu^t \|\mathbf{z}_{\text{ref}}\|d\nu\Big)\\
&< \exp\Big(-2\sigma_{\text{m}}(t-\nu) + 4L_{\partial\mathbf{f}}(1 + L_\eta^{va})\gamma(t-\nu)\\
&\qquad + 2L_{\partial\mathbf{f}}B_\eta^{va}(t-\nu) + 2L_{\partial\mathbf{f}}\varepsilon(T)(t-\nu) + 2L_{\partial\mathbf{f}}\rho_{\text{ref}}T\Big)\\
&= \exp\left(-2\sigma_{\text{m}}(t-\nu) + 2k(T)(t-\nu) + 2L_{\partial\mathbf{f}}\,\rho_{\text{ref}}T\right)\\
&= \xi\,\exp\left(\bar{\lambda}(t-\nu)\right),
\end{aligned}$$

with $\varepsilon(t)$, $\bar{\lambda}$ and ξ defined in (76), (79) and (78). Due to condition (77), we know that $\sigma_{\text{m}} > k(T)$ and thus

$$V_e < \frac{\xi\gamma\bar{\gamma}_0}{|\bar{\lambda}|}\|\mathbf{B}\|B_{\text{CHe}} + \frac{\xi\gamma^2}{|\bar{\lambda}|}\bar{k}L_\eta^{va} + \underbrace{\xi\int_0^t e^{\bar{\lambda}(t-\nu)}\mathbf{e}'\mathbf{B}(\boldsymbol{\phi}_2 + \boldsymbol{\phi}_3)d\nu}_{V_n}\,. \tag{109}$$

The term V_n in (109) is the solution for

$$\begin{aligned}
&\dot{V}_n = \bar{\lambda}\,V_n + \mathbf{e}'[\mathbf{B}_v\mathbf{B}_\omega]\,[\boldsymbol{\chi}'_v\boldsymbol{\chi}'_\omega]'\,,\ V_n(0) = 0\,,\\
&\boldsymbol{\chi}_k(s) = (\mathbf{I}_{3\times 3} - \mathbf{C}_k(s))(\mathfrak{L}[\boldsymbol{\sigma}_{ka} - \boldsymbol{\sigma}_{ka,\text{ref}}\\
&\qquad + \tilde{\boldsymbol{\kappa}}_k\hat{\boldsymbol{\kappa}}_k^{-1}(\boldsymbol{\sigma}_{kn} - \boldsymbol{\sigma}_{kn,\text{ref}})])\,,\ k \in \{v, \omega\}\,.
\end{aligned}$$

With Lemma 3 and the fact that $\|\dot{\boldsymbol{\sigma}}_{kl} - \dot{\boldsymbol{\sigma}}_{kl,\mathrm{ref}}\| \leq L_{\dot{\sigma}}^{kl}\gamma$ and $\boldsymbol{\sigma}_{kl}|_{t=0} = \boldsymbol{\sigma}_{kl,\mathrm{ref}}|_{t=0}$ we obtain

$$\|V_n\| \leq r_e := \frac{\gamma^2}{|\bar{\lambda}|}\sum_{k=v}^{\omega}\|\mathbf{B}_k\|\,\|\mathbf{G}_k(s)\|_{\mathcal{L}_1}(L_{\dot{\sigma}}^{ka} + B_{\bar{\kappa}}^{k}L_{\dot{\sigma}}^{kn}). \quad (110)$$

Inserting (110) into (109) yields with (50)

$$\begin{aligned} V_{\mathrm{e}} &< \frac{\xi\gamma\bar{\gamma}_0}{|\bar{\lambda}|}\,\|\mathbf{B}\|\,B_{\mathrm{CHe}} + \frac{\xi\gamma^2}{|\bar{\lambda}|}\bar{k}L_{\boldsymbol{\eta}}^{va} + \xi\, r_e \\ &= \frac{1}{2}c_0\gamma\bar{\gamma}_0 + \frac{1}{2}c_1\gamma^2 = \frac{1}{2}(c_0 g_0 + c_1)\gamma^2, \end{aligned} \quad (111)$$

where c_0 and c_1 are defined in (78) and (79). Due to the conditions (79), we have

$$\|\mathbf{e}\| < \gamma, \quad (112)$$

which contradicts the first assumption in (101) and proves (86). This result combined with (102) proves the bound (82) and Lemma 2 applied for $t \geq 0$ leads to (85). Further, it follows from (45) and (61) that

$$\begin{bmatrix}\mathbf{T}_d \\ \boldsymbol{\tau}\end{bmatrix} = \begin{bmatrix}\mathbf{T}_{d,\mathrm{ref}} \\ \boldsymbol{\tau}_{\mathrm{ref}}\end{bmatrix} + \hat{\boldsymbol{\kappa}}^{-1}(\boldsymbol{\sigma}_{n,\mathrm{ref}} - \boldsymbol{\sigma}_n) + \boldsymbol{\kappa}^{-1}(\boldsymbol{\eta}_{a,\mathrm{ref}} - \hat{\boldsymbol{\eta}}_a). \quad (113)$$

With (73), (74), (87), (88) and (113), we can finally verify the results (83) and (84).

Acknowledgement: We like to thank F. Holzapfel, T. Raffler and J. Wang from the Institute of Flight System Dynamics of the TU München and especially T. H. Go, W. Zhao and S. H. Chiew from the School of Mechanical & Aerospace Engineering of the Nanyang Technological University in Singapore for their kind support.

The research of P. De Monte is supported by the German Federal Ministry of Economics and Technology.

Received April 30, 2013; accepted November 1, 2013.

References

1. K.J. Aström and B. Wittenmark. *Adaptive control*. Dover Publications, Inc., 2008.
2. A. Datta and Ming-Tzu Ho. On modifying model reference adaptive control schemes for performance improvement. *IEEE Transactions on Automatic Control*, 39:1977–1980, 1994.
3. A. Datta and P.A. Ioannou. Performance analysis and improvement in model reference adaptive control. *IEEE Transactions on Automatic Control*, 39:2370–2387, 1994.
4. I. Fantoni and R. Lozano. *Non-linear Control for Underactuated Mechanical Systems*. Springer, 2002.
5. E. Frazzoli, M.A. Dahleh, and E. Feron. Trajectory tracking control design for autonomous helicopters using a backstepping algorithm. In *Proceedings of the American Control Conference*, 2000.
6. O. Fritsch, P. De Monte, M. Buhl, and B. Lohmann. Quasi-static feedback linearization for the translational dynamics of a quadrotor helicopter. In *Proceedings of the American Control Conference*, pages 125–130, 2012.
7. B.J. Guerreiro, C. Silvestre, R. Cunha, C. Cao, and N. Hovakimyan. L1 adaptive control for autonomous rotorcraft. In *Proceedings of the American Control Conference*, 2009.
8. T. Hamel, R. Mahony, R. Lozano, and J. Ostrowski. Dynamic modelling and configuration stabilization for an X4-Flyer. In *Proceedings of the 15th IFAC World Congress*, 2002.
9. J. Hauser, S. Sastry, and G. Meyer. Nonlinear control design for slightly non-minimum phase systems: Application to V/STOL aircraft. *Automatica*, 28:665–679, 1992.
10. N. Hovakimyan and C. Cao. *L1 Adaptive Control Theory: Guaranteed Robustness With Fast Adaptation*. SIAM – Society for Industrial and Applied Mathematics, 2010.
11. N. Hovakimyan, C. Cao, E. Kharisov, E. Xargay, and I.M. Gregory. L1 adaptive control for safety-critical systems. *IEEE Control Systems Magazine*, 31:54–104, 2011.
12. T.J. Koo and S. Sastry. Output tracking control design of a helicopter model based on approximate linearization. In *Proceedings of the 37th IEEE Conference on Decision and Control*, 1998.
13. M. Krstic, I. Kanellakopoulos, and P. Kokotovic. *Nonlinear and Adaptive Control Design*. John Wiley & Sons, Inc., 1995.
14. D. Lee, H. Jin Kim, and S. Sastry. Feedback linearization vs. adaptive sliding mode control for a quadrotor helicopter. *International Journal of Control, Automation, and Systems*, 7:419–428, 2009.
15. D. Lee, C. Nataraj, T.C. Burg, and D.M. Dawson. Adaptive tracking control of an underactuated aerial vehicle. In *Proceeding of the American Control Conference*, 2011.
16. T. Lee, M Leoky, and N. H. McClamroch. Geometric tracking control of a quadrotor UAV on SE(3). In *Proceedings of the 49th IEEE Conference on Decision and Control*, 2010.
17. R. Mahony and T. Hamel. Adaptive compensation of aerodynamic effects during takeoff and landing manoeuvres for a scale model autonomous helicopter. *European Journal of Control*, 7:1–15, 2001.
18. A. Roberts and A. Tayebi. Adaptive position tracking of VTOL UAVs. *IEEE Transactions on Robotics*, 27:129–142, 2011.
19. J. Sun. A modified model reference adaptive control scheme for improved transient performance. *IEEE Transactions on Automatic Control*, 38:1255–1259, 1993.
20. X. Wang and N. Hovakimyan. L1 adaptive controller for nonlinear time-varying reference systems. *Systems & Control Letters*, 61:455–463, 2012.
21. B.E. Ydstie. Transient performance and robustness of direct adaptive control. *IEEE Transactions on Automatic Control*, 37:1091–1105, 1992.

Dipl.-Ing. Paul De Monte
Lehrstuhl für Regelungstechnik,
Technische Universität München, Fakultät Maschinenwesen, Boltzmannstr. 15,
D-85748 Garching bei München, Fax:
+49-(0)89-289-15653
paul.demonte@tum.de

Dipl.-Ing. Paul De Monte arbeitet am Lehrstuhl für Regelungstechnik im Bereich nichtlinearer adaptiver Trajektorienfolgeregelungen für Quadrokopter.

Prof. Dr.-Ing. habil. Boris Lohmann
Lehrstuhl für Regelungstechnik,
Technische Universität München, Fakultät Maschinenwesen, Boltzmannstr. 15,
D-85748 Garching bei München, Fax:
+49-(0)89-289-15653
lohmann@tum.de

Prof. Dr.-Ing. habil. Boris Lohmann ist Leiter des Lehrstuhls für Regelungstechnik der Fakultät Maschinenwesen der TU München. Hauptarbeitsgebiete: Modellreduktion, nichtlineare, robuste und optimale Regelung, aktive Schwingungsdämpfung, industrielle Anwendungen.